2/8/2012

U.S.NRC
United States Nuclear Regulatory Commission
Protecting People and the Environment

NUREG/CR-XXXX
PNNL-XXXXX

Ultrasonic Phased Array Assessment of the Interference Fit and Leak Path of the North Anna Unit 2 Control Rod Drive Mechanism Nozzle 63 with Destructive Validation

Office of Nuclear Regulatory Research

B|20

U.S.NRC
United States Nuclear Regulatory Commission
Protecting People and the Environment

NUREG/CR-XXXX
PNNL-XXXXX

Ultrasonic Phased Array Assessment of the Interference Fit and Leak Path of the North Anna Unit 2 Control Rod Drive Mechanism Nozzle 63 with Destructive Validation

Manuscript Completed: January 2012
Date Published:

Prepared by
S. L. Crawford, A. D. Cinson, P. J. MacFarlan, B. D. Hanson,
R. A. Mathews

Pacific Northwest National Laboratory
P.O. Box 999
Richland, WA 99352

G. Oberson, NRC Project Manager

NRC Job Code N6783

Office of Nuclear Regulatory Research

Abstract

In this investigation, nondestructive and destructive testing methods were employed to evaluate potential boric acid leakage paths through an Alloy 600 control rod drive mechanism (CRDM) penetration, Nozzle 63, from the North Anna Unit 2 power plant that was removed from service in 2002. A previous ultrasonic examination of this nozzle, conducted during an in-service inspection (ISI) prior to the head removal, identified a probable leakage path in the interference fit between the penetration and the vessel head. Subsequently, Nozzle 63 was made available for independent testing. Nozzle 63 was examined using phased-array ultrasonic testing with a 5.0-MHz, eight-element annular array; immersion data were acquired from the nozzle inner diameter surface. Responses from a mock-up specimen were initially evaluated to determine detection limits and characterization capability of the probe as well as to identify and assess differences in ultrasonic responses with and without the presence of boric acid in the interference fit region. The ultrasonic evaluation of Nozzle 63 found a primary leak path as well as other partial leak paths. Following the nondestructive examination, Nozzle 63 was destructively examined to visually assess the leak paths. Additional thickness measurements were made on the boric acid deposits on the reactor pressure vessel head. These destructive and nondestructive results are compared and the results are presented. The results of this investigation may be used by the NRC to evaluate licensees' volumetric leak path assessment methodologies and to support regulatory inspection requirements.

Foreword

(To be written by Greg - NRC.)

Contents

Comment [PGO1]: Update table of contents to reflect any changes

Figures

Comment [PG02]: Update list to reflect any changes.

Tables

Executive Summary

Research is being conducted for the U.S. Nuclear Regulatory Commission (NRC) at the Pacific Northwest National Laboratory (PNNL) to assess the effectiveness and reliability of advanced nondestructive examination (NDE) methods for the detection and characterization of flaws in nuclear power plant components. One area of concern is in primary water stress corrosion cracking (PWSCC) in the nickel-base alloys used in primary pressure boundary components in pressurized water reactors (PWRs). Nickel-based alloys exposed to reactor coolant in PWRs may experience a form of degradation known as PWSCC. One PWR component that has an operational history of PWSCC is the control rod drive mechanism (CRDM) nozzle. The CRDM nozzles are cylindrical penetrations in the upper reactor pressure vessel (RPV) head that allow for the insertion and removal of control rods. The penetration tube is held in place with an interference fit, and is seal-welded to the vessel head with a J-groove weld. Cracking in the nozzle or weld metal can allow borated water to leak to the top of the RPV head. Corrosion of the RPV head is a concern, as was discovered at Davis Besse, as well as nozzle ejection in the presence of extensive circumferentially oriented cracking. In response to the repeated occurrence of RPV head leakage, licensees were directed to perform a "demonstrated" surface or volumetric leak path assessment of all J-groove welds in the RPV head.

The original construction materials for the CRDM nozzles at North Anna 2 were Alloy 600 base metal and Alloy 82/182 weld metal. During the Fall-2001 refueling outage, coolant leakage was noted near Nozzle 63. NDE showed crack-like indications near the J-groove weld and butter layer in the nozzles and shallow axial cracking on the inner diameter. The leaking welds were repaired with Alloy 52/152 material, thought to have higher PWSCC resistance than Alloy 82/182. Subsequent visual examination of the RPV head in the Fall-2002 outage again revealed leaking nozzles. The head was replaced and several nozzles including Nozzle 63 became available for study. The purpose of this investigation was to confirm features previously identified by industry in an ultrasonic evaluation with an equivalent or better examination and to validate the findings by opening the nozzle assembly to reveal the annulus surfaces.

This study resulted in a successful ultrasonic examination of the interference fit region of control rod drive mechanism Nozzle 63 from the North Anna Unit 2 power plant. A phased-array ultrasonic system was calibrated on a mockup specimen containing two interference fit regions. The probe spot size at the interference fit was modeled at 1.2 by 1.2 mm (0.04 by 0.04 in.) at the −6 dB level. Ultrasonic data from notches in the carbon steel material from one of the mockup interference fit regions showed system resolution at nominally 4 mm (0.16 in.) in both the axial and circumferential directions. Notches as shallow as 0.028 mm (0.0011 in.) were detected as well as notches as narrow as 0.80 mm (0.10 in.) in the circumferential direction. The second interference fit mockup contained regions with boric acid deposits. These regions were ultrasonically imaged and suggested that the ultrasonic responses could be segmented into three categories: 1) good interference fit, 2) interference fit with boric acid, and 3) leak path or gap.

Ultrasonic data were acquired on Nozzle 63 and clearly showed a variation of responses throughout the annulus region. The primary leak path at the downhill position of the nozzle was imaged and definitively spanned the annulus region, thus providing a path for borated water to

reach the top of the head. Partial leak paths were also identified. The normal beam inspection, while not optimum for crack detection, also detected two axial cracks in the nozzle. These cracks were previously found by industry with an eddy current examination conducted during an in-service inspection. One of the cracks was below the weld at the uphill position. The other axial crack was located above the weld at the downhill position, which also places it in the main leak path. A comparison of the PNNL ultrasonic images to data obtained by industry showed similar results, but the PNNL data had better resolution, data registration, and focusing. Finally, a supplemental evaluation of the weld, which was again not optimized for crack detection, failed to detect any weld cracking but did detect numerous near-surface fabrication flaws.

After sectioning of the nozzle assembly to reveal the interference fit and photographing the exposed surfaces, the primary leak path was confirmed. Also confirmed was the excellent agreement of the ultrasonic images and revealed features on the annulus surfaces.

Additional measurements were made to quantify the thickness of the boric acid deposits or corrosion layer on the RPV head. It was reasonable to assume that any gap in the annulus could fill with boric acid deposits. As the gap between Alloy 600 tube and low-alloy steel head varied so too did the boric acid thickness. The leak path or bare metal corrosion layer throughout the annulus was 16 microns (0.63 mils) or less with ultrasonic responses greater than 65%. Boric acid apparently did not deposit in the leak path due to the constant flow of borated water through the area, and the ultrasonic response indicates an air gap was present. The boric acid deposits in the counter bore regions above and below the interference fit were in the 132 to 192 micron (5.2 to 7.6 mils) range with ultrasonic responses between 48 and 83%. These two regions, leak path and counter bore, are clearly distinct from each other in both boric acid thickness but overlap in ultrasonic response. The interference fit region with a narrower annulus had boric acid deposits in the 16 to 75 micron (0.63 to 3.0 mils) range, in between the leak path and counter bore values. There was not a direct correlation between the RPV head boric acid measurements in the interference fit region and the ultrasonic responses. This is not unexpected as the ultrasound was influenced by additional physical conditions that were not measured such as the deposits on the outside of the Alloy 600 tube surface and the density of any of the deposits.

Lastly, the leak path region of the RPV head was replicated and limited confirmatory measurements made on the replica for boric acid thickness. The replica surfaces were imaged with a stereomicroscope and showed minor evidence of corrosion product streaking and little or no corrosion or wastage. Machining marks were clearly evident across the main leak path. Two small areas with minor corrosion were found above the main leak path with depths of 0.25 mm (0.01 in.). Attempts to remove the boric acid deposits on the RPV head to determine wastage underneath were unsuccessful, but dental pick probing indicated that all areas were sound. Therefore, in this leaking nozzle assembly, there was minimal corrosion or wastage occurring on the low-alloy steel RPV head.

Acknowledgments

The work reported here was sponsored by the U.S. Nuclear Regulatory Commission (NRC) and conducted under NRC Job Code Number N6783. Greg Oberson is the NRC project manager. The Pacific Northwest National Laboratory (PNNL) would like to thank Dr. Oberson, Mr. Darrell Dunn and Mr. Jay Collins for their guidance throughout the course of this effort.

The authors acknowledge and thank J. W. Hyres, et al. at Babcock & Wilcox Technical Services Group in Lynchburg, Virginia, for cutting the nozzle assembly, for acquiring additional measurements on the head material, and for excellent photography and documentation of their work. A special thanks to Jim for his flexibility and willingness to try new approaches to obtain requested data is due.

The authors acknowledge and thank John P. (Jack) Lareau from WesDyne International for providing information on in-service inspections (ISI) and nozzle fabrication as well as data from an ISI on Nozzle 63.

The authors also thank Kay Hass for her diligence and patience in editing and preparing the manuscript.

PNNL is operated by Battelle for the U.S. Department of Energy under Contract DE-AC05-76RL01830.

Acronyms and Abbreviations

ASME	American Society of Mechanical Engineers
BW	bandwidth
B&W	Babcock and Wilcox Technical Services Group
CASS	cast austenitic stainless steel
CCSS	centrifugally cast stainless steel
CFR	Code of Federal Regulations
COD	crack opening dimension
CRDM	control rod drive mechanism
CWD	constant wedge delay
dB	decibels
EDM	electric discharge machining
EPRI	Electric Power Research Institute
FSH	full screen height
ID	inner diameter
IR	infrared
ISI	inservice inspection
LN	liquid nitrogen
LWR	light water reactor
NDE	nondestructive examination
NPP	nuclear power plant
NRC	U.S. Nuclear Regulatory Commission
OD	outer diameter
PA	phased array
PA-UT	phased array ultrasonic testing
PDI	performance demonstration initiative
PE	pulse-echo
PNNL	Pacific Northwest National Laboratory
PT	liquid penetrant testing
PWR	pressurized water reactor
PWSCC	primary water stress corrosion cracking
PZR	pressurizer
RMSE	root mean square error
RPV	reactor pressure vessel
RT	room temperature
RVH	reactor vessel head
SNR	signal-to-noise ratio

TLR	technical letter report
TOFD	time-of-flight diffraction
TRL	transmit-receive longitudinal
UT	ultrasonic testing

1 Introduction

Research is being conducted for the U.S. Nuclear Regulatory Commission (NRC) at the Pacific Northwest National Laboratory (PNNL) to assess the effectiveness and reliability of advanced nondestructive examination (NDE) methods for the detection and characterization of flaws in nuclear power plant components. One area of concern is in primary water stress corrosion cracking (PWSCC) in the nickel-base alloys used in primary pressure boundary components in pressurized water reactors (PWRs). Nickel-based alloys exposed to reactor coolant in PWRs may experience a form of degradation known as PWSCC. One PWR component that has an operational history of PWSCC is the control rod drive mechanism (CRDM) nozzle. As shown in Figure 1.1, the CRDM nozzles are cylindrical penetrations in the upper reactor pressure vessel (RPV) head that allow for the insertion and removal of control rods. The penetration tube is held in place with an interference fit, represented as the area between the two horizontal dashed lines in the figure labeled 'shrink fit zone', and is seal-welded to the vessel head with a J-groove weld. Counter bore regions are not designed to be compression-fit zones between the nozzle and RPV head and are shown exaggerated in the drawing. Most CRDM nozzles originally placed into service in PWRs were fabricated from the nickel-based alloy referred to as Alloy 600, along with the Alloy 82 and 182 weld metals. PWSCC of a CRDM nozzle in a PWR was first identified in the Bugey Unit 3 plant in France during an over-pressurization test in 1991 (Economou et al. 1994). The crack initiated in the Alloy 600 base metal and propagated into the Alloy 182 weld metal. In late 2000 and early 2001, reactor coolant leakage to the RPV head from axial through-wall cracks in CRDM nozzles was identified at Arkansas Nuclear One Unit 1 and Oconee Unit 1 (Grimmel 2005). Follow-up inspections at Oconee Units 2 and 3 in 2001 identified axial and circumferentially oriented cracks. The circumferentially oriented cracks were of particular concern because of the possibility of nozzle ejection.

Leakage of borated water to the RPV head may occur as cracks initiate on the J-groove weld surface, propagate through the weld to the triple point, and allow water into the annulus region between the nozzle outer diameter (OD) and the RPV head. The triple point is diagrammed in Figure 1.2 and is the point at which the RPV head, buttering, and Alloy 600 CRDM tube meet. Once the boundary formed by an intact J-groove weld is compromised, there is the potential for a leakage path through the interference fit allowing reactor coolant to reach the outer surface of the RPV. The coolant can flash to steam, leaving boric acid deposits on the head and in the interference fit region around the leakage path. Additionally, a steam-cut leakage path through the interference fit and annulus may also be produced at operating temperature and pressure in a plant when a gap in the carbon steel RPV head at the uphill and downhill positions opens due to material expansions.

In response to the discovery of the CRDM cracks at Oconee Unit 3, in August 2001, the NRC issued Bulletin 2001-01, "Circumferential Cracking of Reactor Pressure Vessel Head Penetration Nozzles." PWR licensees were directed to evaluate the susceptibility of head penetration nozzles to PWSCC and to provide inspection plans to detect potential cracking. Thereafter, CRDM cracking was identified at additional PWRs including Davis Besse (Bennetch et al. 2002) and North Anna Unit 2 (NRC 2002). At Davis Besse, reactor coolant leakage led to significant wastage of carbon steel in a portion of the RPV head, leaving only a layer of stainless steel cladding at the pressure boundary. In response to the repeated occurrence of RPV head leakage, in 2004 NRC issued EA-03-009 for PWR licensees requiring additional periodic inspections and evaluation of boric acid deposits as they pertain to the reasonable assurance of plant operational safety. The requirements of EA-03-009 were superseded by the adoption of American Society of Mechanical Engineering (ASME) Section XI Code Case N-729-1 by rulemaking in Title 10 of the Code of Federal Regulations (10 CFR) Part 50.55(a)(g)(6)(ii)(D)(1). As a condition in 10 CFR 50.55(a)(g)(6)(ii)(D)(3), licensees are directed to perform a "demonstrated" surface or volumetric leak path assessment of all J-groove welds in the RPV head.

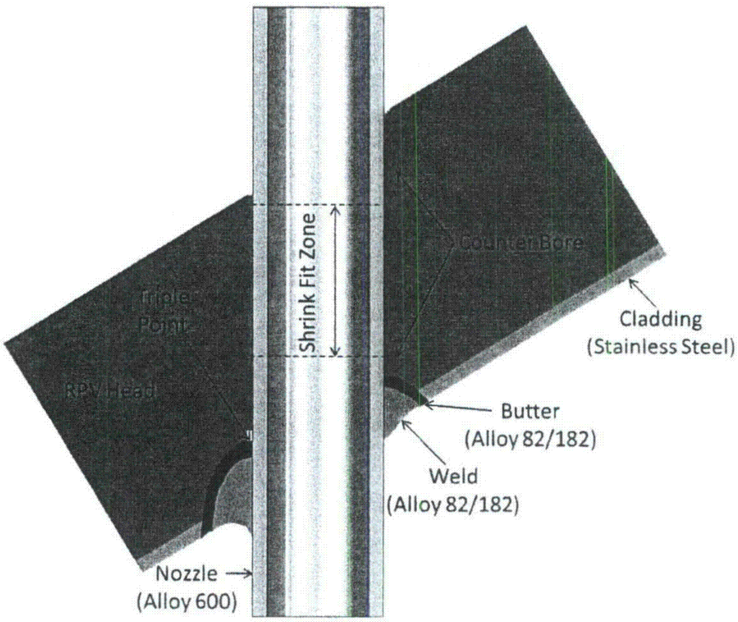

Figure 1.1 CRDM J-groove Weld Schematic

Comment [PG03]: Why doesn't the shrink fit go down to the top of the J-groove weld?

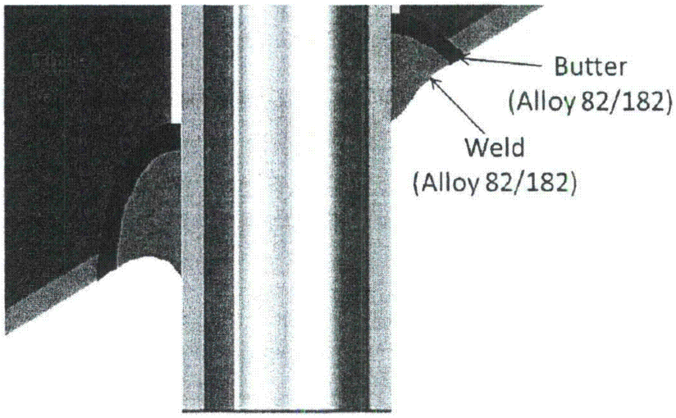

Figure 1.2 The Triple Point in the Assembly Where the Alloy 600 Nozzle, RPV Head, and Buttering Material Meet

A leak path assessment involves the use of an NDE technique, such as ultrasonic testing (UT), to determine whether a flow path exists through the interference fit that would allow reactor coolant to access the outside of the RPV head. The ultrasonic response from the interference fit examination will likely detect a leak path and may additionally detect corrosion or loss of material as well as the presence of boric acid in the annulus region. Industry groups, such as the Electric Power Research Institute (EPRI), are participating in programs to generically demonstrate the volumetric leak path assessment. As part of this initiative, EPRI obtained CRDM nozzles removed from operational service at the North Anna Unit 2 plant for further analysis and testing. North Anna Unit 2 is a three-loop Westinghouse PWR that was placed into service in 1980. The materials of construction for the original CRDM nozzles were Alloy 600 base metal and Alloy 82/182 weld metal.

Visual inspection of the outer surface of the North Anna Unit 2 RPV head during the Fall-2001 refueling outage indicated reactor coolant leakage in the proximity of penetrations 51, 62, and 63 as evinced by the presence of boric acid crystals (EPRI 2005). NDE of the nozzles showed crack-like indications near the J-groove weld/butter layer in the nozzles and shallow axial cracking on the inner diameter. The leaking welds in these nozzles were repaired using a temper bead repair technique with nickel-based Alloys 52 and 152, which are thought to have higher PWSCC resistance than Alloy 182. Subsequent visual examination of the RPV head during the Fall-2002 outage revealed 6 CRDM nozzles that were suspected of leaking and 21 that were masked to the extent that their status could not be determined. Eddy current and ultrasonic examinations showed numerous axial and circumferential indications in the nozzles, including those repaired during the previous outage. Given the extensive degradation of the RPV head, the utility made the decision to replace the head during the 2002 outage and make it available for further examination and study. EPRI took possession of six CRDM nozzles from the removed head including nozzles 10, 31, 51, 54, 59, and 63, which were transferred to

PNNL. Several of these nozzles were subsequently studied by EPRI and the NRC including nozzles 10, 31, 54, and 59 (EPRI 2006; Cumblidge et al. 2009).

The subject of this report is a leak path assessment of Nozzle 63 from North Anna Unit 2. This nozzle is of additional interest because of the Alloy 52/152 weld repair during the Fall-2001 outage. The purpose of this investigation is to determine whether features identified by a UT examination of the nozzle, including leak paths, voids, and the presence of boric acid in the interference fit, are confirmed by destructive analysis. The UT process is assumed to be equivalent to or better than that used in industry examinations. The radiological and mechanical steps taken to configure the nozzle for the ultrasonic evaluation are discussed in Section 2. Section 3 presents technical information on the ultrasonic transducer, the system electronics, and mechanical scanner. The calibration mockup specimen is described in Section 4 and consists of a notched specimen and a specimen with boric acid in the interference fit. Ultrasonic data on the mockup specimens are presented and system resolution and flaw detection capabilities are discussed. The ultrasonic evaluation of Nozzle 63 and corresponding results are presented in Section 5. Section 6 documents the cutting activities on the nozzle assembly to reveal the interference fit. Initial views of the annulus region are shown. Section 7 compares the ultrasonic findings to the visual evaluation of the interference fit. An ultrasonic weld examination for fabrication flaws and cracking was conducted and is described in Section 8. Section 9 contains additional measurements on the RPV head including boric acid thickness measurements in the annulus and Microset replica measurements of the primary leak path region. Lastly, a summary of the finding is presented in Section 10 and conclusions that can be drawn at this time. Section 11 gives references cited in this report.

2 Nozzle Preparation

When received at the Pacific Northwest National Laboratory (PNNL), the control rod drive mechanism (CRDM) Nozzle 63 from the North Anna Unit 2 reactor consisted of a flame cut section of the upper reactor pressure vessel (RPV) head and a full length Alloy 600 penetration tube, as shown in Figure 2.1. The CRDM was removed from its storage box and a radiologic survey performed. The flame cut edges of the CRDM were then painted with two coats (the first yellow, the second red) of a flexible air dried plastic coating from Plasti Dip® to reduce the risk of workers being cut while handling the CRDM (see Figure 2.2). An expandable 3-in. plug was inserted in the wetted-side of the penetration tube so the tube could be filled with water. In retrospect, it would have been better to cut the nozzle prior inserting the plug. This may have reduced some of the debris that first coated the ultrasonic scanner (see Section 5.2). With the plug inserted, the nozzle was wrapped in plastic (see Figure 2.3) and bagged to contain contamination during the nozzle cutting. The nozzle was then secured on a wheeled cart that was modified to allow the penetration tube to be kept vertical during the testing, as seen in Figure 2.4.

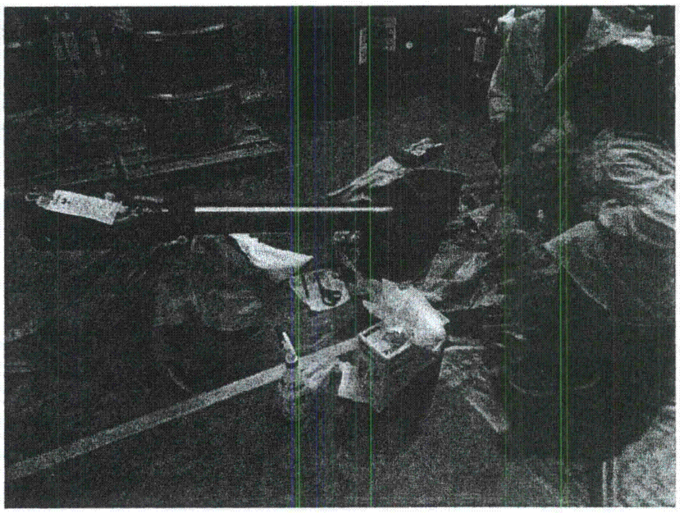

Figure 2.1 As-Received Condition of Nozzle 63.

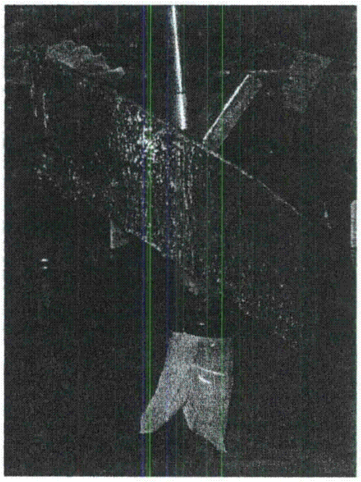

Figure 2.2 Nozzle 63 with Painted Edges.

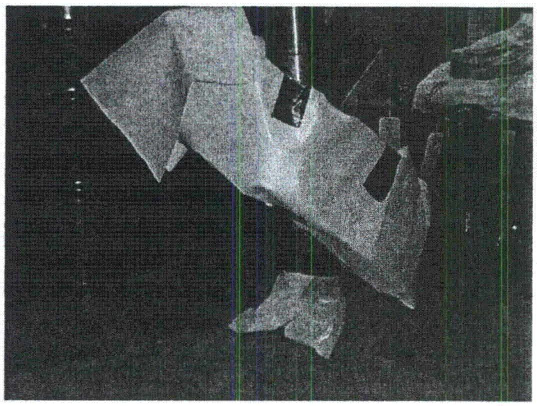

Figure 2.3 Nozzle 63 Wrapped in Plastic for Contamination Control

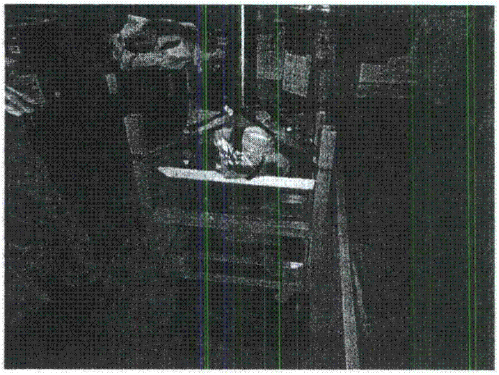

Figure 2.4 Nozzle 63 on Modified Cart

In order to better fit in a glovebag for contamination control purposes and to facilitate connection of the scanner, approximately two feet of the penetration tube had to be removed. A catch pan was first fitted around the penetration tube below where the cut was to be made, approximately 12 in above the RPV steel. A hydraulic rotary pipe cutting tool was then fitted around the penetration tube as shown in Figure 2.5. The penetration tube and catch tray were wrapped in plastic to provide contamination control. The hydraulic cutting tool was connected and the first attempt at cutting the tube was made (see Figure 2.6). A "hard spot" was encountered within the nozzle and two cutting heads broke before the decision was made to attempt a new cut approximately 1 in above the previous cut attempt. Cutting proceeded without any other issues in this new location. The removed section of the penetration tube was placed in a 55 gallon drum for storage.

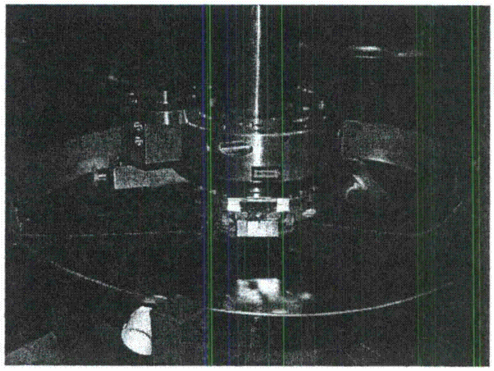

Figure 2.5 Nozzle 63 with Hydraulic Rotary Pipe Cutting Tool

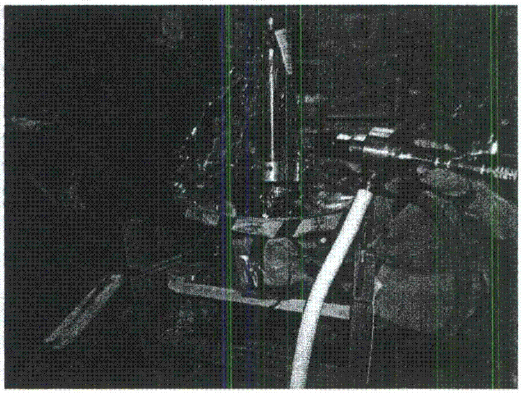

Figure 2.6 Cutting of Nozzle 63 Penetration Tube.

After cutting, the CRDM was completely wrapped in plastic to prevent the spread of contamination. The CRDM was then transported to RPL/33 where a containment glovebag had been assembled to house the nozzle. The cart with the nozzle was wheeled into the glovebag as shown in Figure 2.7. Once the nozzle was properly positioned, the two-axis scanner with attached ultrasonic phased array probe was lowered through an upper access port and centered onto the penetration tube. The scanner was secured to the penetration tube using three set screws. The main door and the upper access port were sealed and the control cables secured to the upper frame. Approximately 1.5 liters of distilled water was added to the penetration tube. The final configuration of the scanner in the glovebag is shown in Figure 2.8.

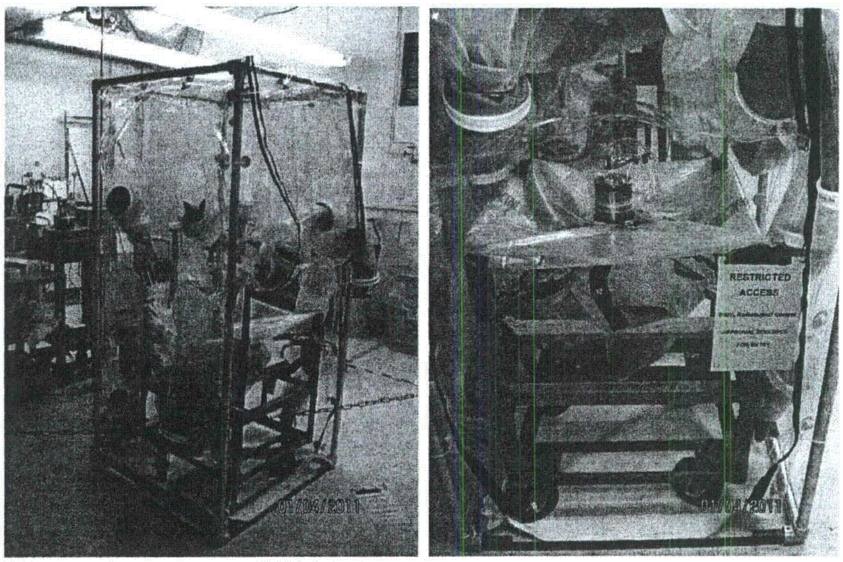

Figure 2.7 CRDM Installed in Containment Glovebag.

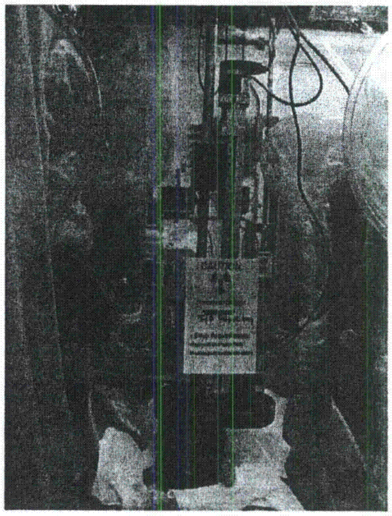

Figure 2.8 Final Configuration of CRDM Nozzle 63 for Examination

3 Ultrasonic Testing Equipment for Nozzle 63 Examination

The nondestructive leak path assessment of Nozzle 63 was performed at the Pacific Northwest National Laboratory (PNNL) with an ultrasonic phased array (PA) probe. A PA probe has multiple individual elements that are electronically fired at prescribed time delays to form a coherent and focused beam at a specified depth in the material under test. The equipment used for this investigation was selected because it is similar to or better than equipment used by industry for in-service inspections of nozzle penetrations in pressurized water reactors (PWRs). A detailed description of the equipment is provided in this section.

3.1 Phased Array Electronics

Ultrasonic data acquisition for Nozzle 63 was accomplished using the ZETEC Tomoscan III phased array system to control the PA probe employed in this study. This commercially available system was equipped to accommodate a maximum of 64 channels of data from PA probes and was operated with UltraVision 1.2R4 software. Its frequency pulsing electronics can drive probes in the 0.7–20 MHz range. The system is capable of accepting multiple axis positional information from external encoders to map ultrasonic data to spatial location on a specimen. The data acquisition system is shown in Figure 3.1.

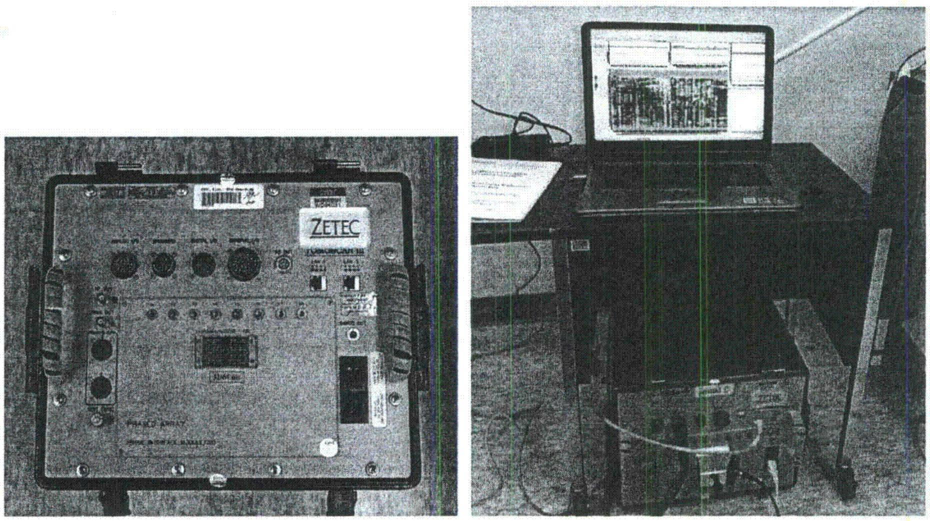

Figure 3.1 Data Acquisition System and Laboratory Workstation. Left: Tomoscan III phased array data acquisition system. Right: Laboratory workstation/laptop computer for both data acquisition and data analysis, with the Tomoscan III system below.

3.2 Phased Array Probe and Software Simulations

Nozzle 63 was examined with a pulse-echo (PE) longitudinal-wave immersion phased-array probe with a center frequency of 5 MHz, as shown in Figure 3.2. The PA probe was designed in a 1-D annular configuration using eight elements. The probe contained elements in a Fresnel radius pattern starting with a radius of 3 mm (0.12 in.) up to the final element radius of 9.72 mm (0.38 in.). Thus, the total aperture was 296.81 mm^2 (0.46 in.^{2}). As characterized by the manufacturer, Imasonic, the probe exhibited an overall 71% bandwidth at −6 decibels (dB) with all eight elements and an overall central frequency of 5.4 MHz. This design was chosen for enhanced depth focusing capabilities. Its beam-forming capabilities showed a satisfactory insonification of the interference fit region of interest as well as the ability to propagate a coherent ultrasonic beam deep into the weld region. Figure 3.3 shows the probe attached to the scanning arm.

Before the PA probe was used for the examination, a set of focal laws was produced to control the firing of individual elements. The focal laws were inputs to the UltraVision control software, which determined specific elements to excite at specific times to allow for proper beam-forming in the material. The focal laws may also contain details about insonification angles, the focal depth of the sound field, the delays associated with the wedge and electronics, and the orientation of the probe. For this investigation, a software package contained in the UltraVision software program suite, known as the ZETEC Advanced Focal Law Calculator 1.2R4, was used to produce the focal laws. The software program generated focal laws and simulated the ultrasonic field produced by the probe when using the generated laws. The user entered the physical information about the PA probe and wedge into the program, including the number and size of probe elements, and the wedge angle and size. After the desired angles and focal distances were entered, the software generated the needed delays for each element to produce the desired beam steering and focusing in the material. The software beam simulation produced a simple ray-tracing image of the probe, wedge, and material under evaluation, as well as a density mapping of the modeled sound field. The sound field mapping enabled the user to see how well the sound field was formed with the given input parameters. The probe was also evaluated for the generation of grating lobes that may be detrimental to the examination. It should be noted that the software simulation was performed using an isotropic material assumption; namely, that the velocity of sound is maintained throughout any angle for a particular wave mode. The simulations enabled the user to estimate sound field parameters and transducer performance to optimize array design and focal law development.

Typical control rod drive mechanism (CRDM) nozzles made from Alloy 600 have a tube wall thickness on the order of 15–17 mm (0.59–0.67 in.). The targeted area of interest in this study was the interference fit in the annulus between the nozzle and low alloy steel vessel material. It was important to design a phased array probe capable of depth focusing into this region. Prior to probe fabrication, sound field simulations were conducted using the Phased Array Calculator 1.2R4 software program and the design parameters to simulate a projected sound field into an isotropic material with acoustic properties of Alloy 600. Figure 3.4 shows a side view representation of the focal laws generated on the left and a sound field simulation on the right for a target depth focus of 15 mm (0.59 in.). The gray regions represent the Alloy 600 material and the dark blue regions represent water. In this immersion scanning setup, water was used as the 'wedge' material. The red horizontal line at 15.1 mm (0.59 in.) represents the target focal region. The simulation showed a favorable sound field density at the desired focal depth.

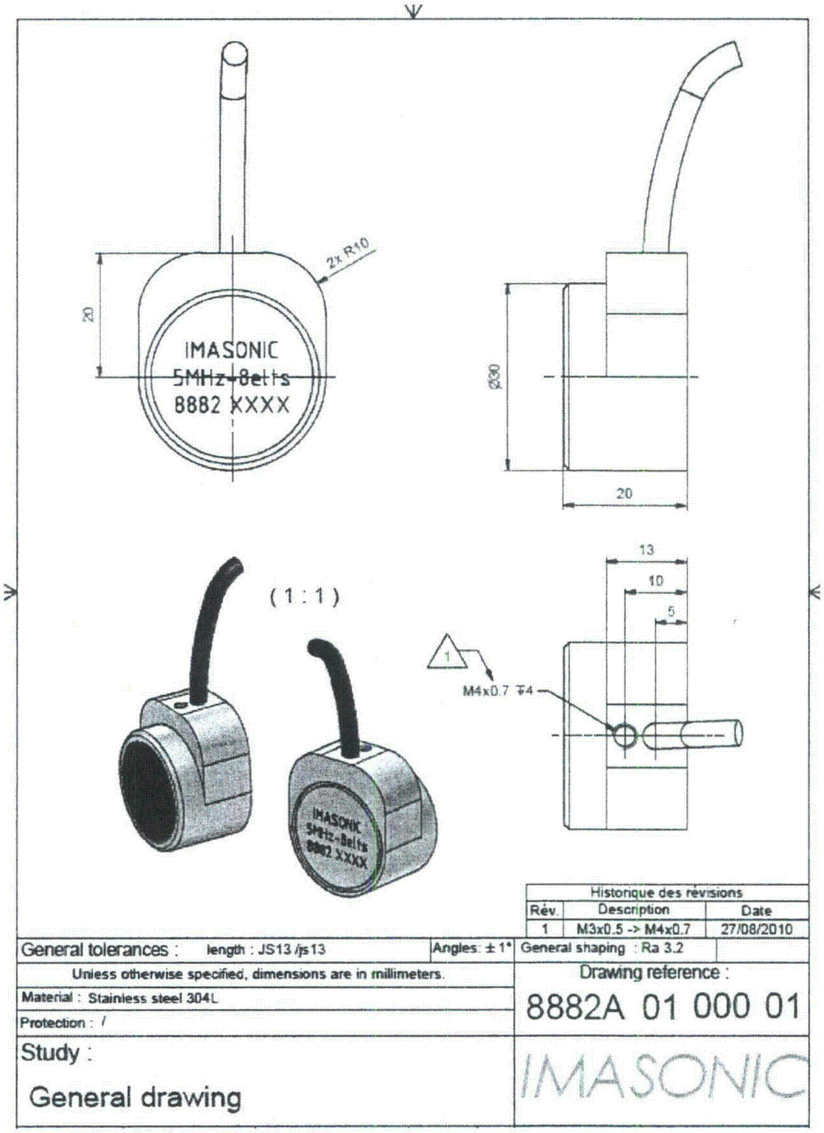

Figure 3.2 5.0-MHz Phased Array Probe

Comment [PGO4]: Do you have (or need) permission to use this figure?

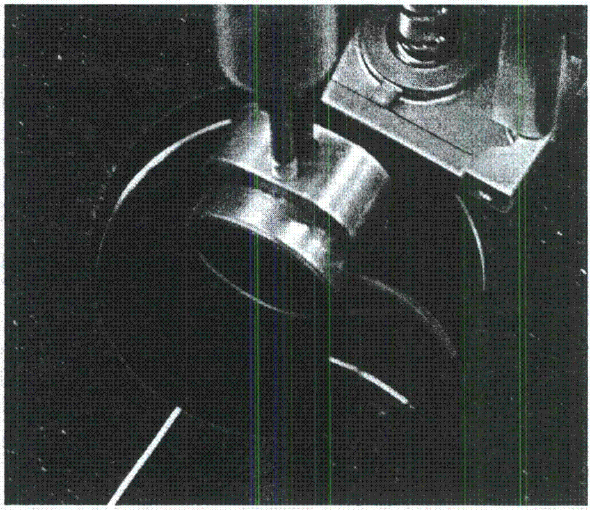

Figure 3.3 Annular Phased Array Probe Attached to Scanner Arm

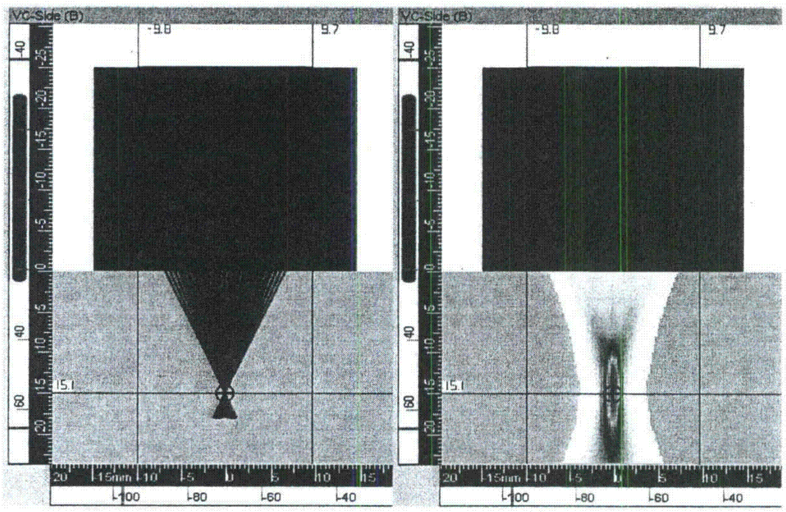

Figure 3.4 Law Formation and Sound Field Simulation for a Depth Focus of 15 mm

Comment [PGO5]: Where is probe in this figure?

The simulations viewed from the top or C-scan view gave information on the overall spot size in the scan and index axes of the formed beam at a particular depth. As seen in Figure 3.5, the predicted –6 dB (50%) and –3 dB (70.7%) spot sizes for the phased array probe focused at a depth of 15 mm (0.59 in.) in Alloy 600 material were 1.2 × 1.2 mm (0.047 × 0.047 in.) and 1.0 × 1.0 mm (0.04 × 0.04 in.), respectively. Additional sound field simulations were modeled at 1 mm (tube inner diameter [ID]) and 30 mm (15 mm into the J-groove weld region). The −6 dB spot size for depth focuses of 1 and 30 mm were 0.6 × 0.6 mm (0.024 × 0.024 in.) and 2.0 × 2.0 mm (0.079 × 0.079 in.), respectively. The −3 dB spot sizes were 0.4 × 0.4 mm (0.016 × 0.016 in.) and 1.4 × 1.4 mm (0.055 × 0.055 in.), respectively.

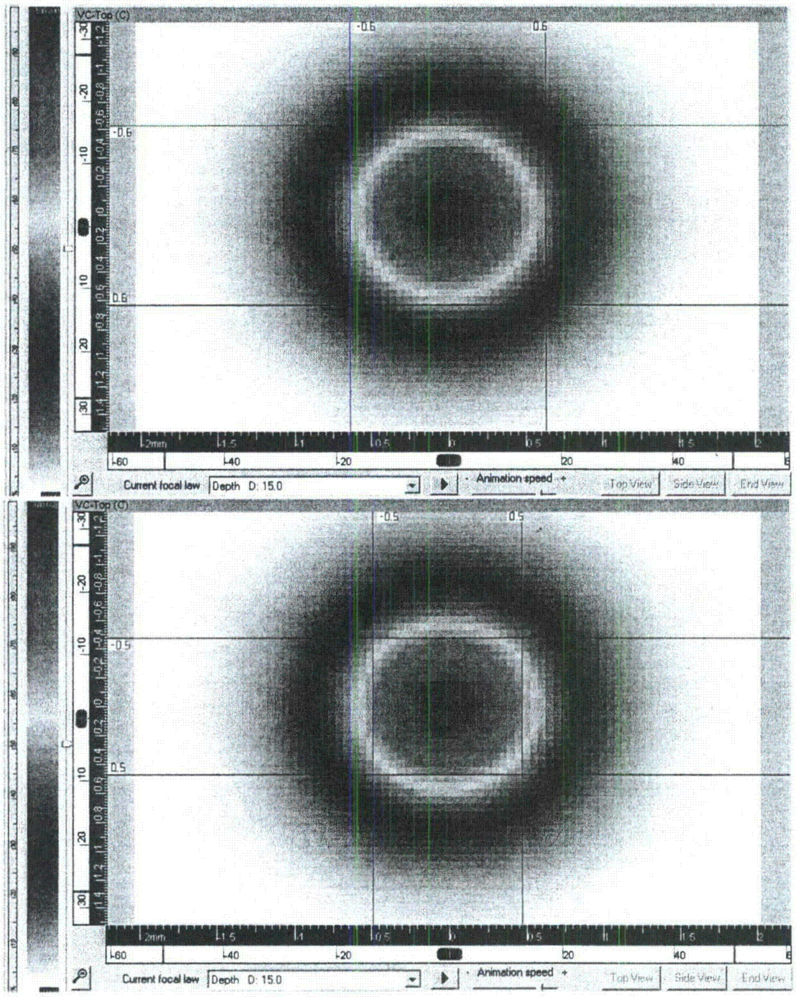

Figure 3.5 **C-Scan View at a Depth Focus of 15 mm. Top: −6 dB spot size. Bottom: −3 dB spot size.**

Comment [PG06]: What is significance of red and blue lines?

3.3 Scanner

The theta-Z scanning apparatus for examining the annulus region of the nozzle from the ID of the penetration tube was constructed by Brockman Precision Machine and Design located in Kennewick, Washington. The ID scanner was designed for inner-surface scanning with ultrasonic probes but could be adapted and used with other sensor technologies. The scanner system was built to attach directly and securely onto the nozzle, centered by three setscrews spaced evenly around the collar of the scanner. Figure 3.6 shows photographs of the scanner sitting on a nozzle mockup specimen. The scanner had a linear, Z or vertical axis for movement along the length of the nozzle and a rotational or theta axis for rotation around the nozzle ID. Motion of the scanner was controlled by two pulse-counter or stepper motors. Optical eye shaft encoders with a sensitivity of 2500 counts per revolution were attached to each motor. The calibrated positional information attained via the slave encoders was routed directly into the ultrasonic system and correlated with the ultrasonic testing (UT) data. The maximum range of motion along the nozzle length was 457.2 mm (18 in.). The rotational motion was continuous with no fixed limits, but was practically constrained to approximately 1.5 revolutions by the cables attached to the motor drivers, encoders, and the PA probe.

The scanner system was controlled using a custom-designed software program interfaced with a pulse-counter motor control system. A menu in the program allowed the user to 'jog' the scanner to a desired position. This feature was useful for setup, mapping the desired scan bounds as well as calibrating the UT signal response at certain locations. The customizable scanning sequence menu allowed the user to specify the scan and index range and resolution settings. Additionally, speed settings were tailored to acquire data with consistency and within the UT data acquisition system limits.

Prior to scanning, the nozzle was arranged in a vertical position, plugged with a water-tight seal in the bottom end, and then filled with distilled water. In immersion scanning, water serves as both the wedge material and the ultrasonic couplant material. The water was given 24 hours or more to degas/de-bubble. Next, the ID of the nozzle specimen was gently brushed to remove bubbles that formed and attached to the ID wall region. Because air bubbles have a strong ultrasonic impedance mismatch to water or steel, it was important to remove them from the ID surface prior to scanning to minimize reflection or distortion of the ultrasonic energy.

The scanner was lowered onto the top of the nozzle specimen, centered, and secured by uniformly tightening the three set screws in the collar. Centering the scanner apparatus allowed the transducer arm to be positioned at the center of the nozzle tube so that a constant sound path was maintained during a circumferential scan sweep to reduce signal walk. The phased array probe was then affixed to the 762-mm (30-in.) scanner arm using an M4 threaded rod running directly into the transducer housing and attached to the vertical axis via a set screw, as shown in Figure 3.7. The transducer face was orientated such that the ultrasonic beam was propagating radially outward towards the annulus or weld region. Using a set screw to hold the scanner arm enabled manual positioning the probe in the vertical axis for increased versatility.

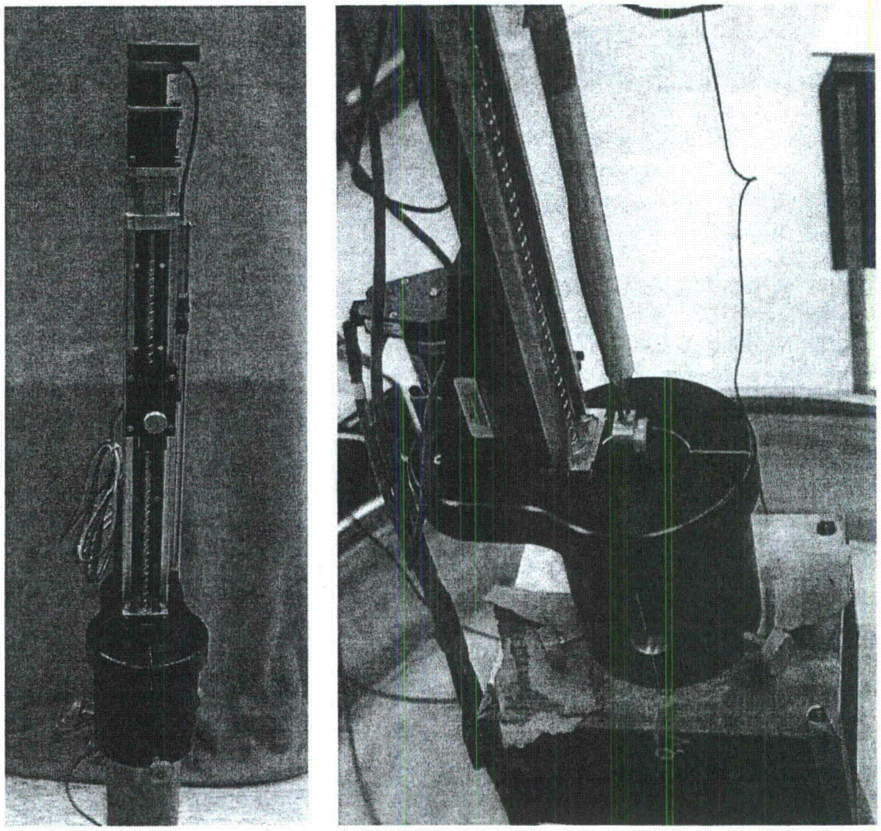

Figure 3.6 Scanner on Mockup Nozzle Specimen. Left: Scanner alone. Right: Scanner with PA probe attached sitting on the calibration mockup specimen.

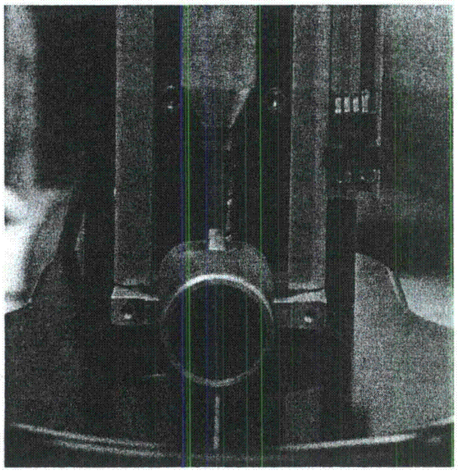

Figure 3.7 Transducer Attachment

The scanning sequence used the rotational or circumferential direction as the scan axis and the vertical direction as the index axis. The positive scan direction was established to be counter clockwise and the positive index was defined as vertically upwards. Positional resolutions were set to 0.25 degrees in the scan and 0.5 mm (0.02 in.) in the index directions for scanning the calibration mockup specimen. For output file size management, Nozzle 63 scanning protocol used 0.5 degrees by 0.5-mm (0.02-in.) resolutions in the scan and index directions, respectively. Figure 3.8 shows a detailed scanning setup schematic on a CRDM nozzle assembly.

Due to the radiation contamination concerns surrounding Nozzle 63, a custom glove bag (details discussed in Section **Error! Reference source not found.**) was constructed to reduce radiation contamination to persons or equipment. Setup in the glove bag required modifications to the glove bag so that scanner and phased array cables and equipment could be passed in while maintaining connection to vital equipment such as the phased array electronics and motor control units. Figure 3.9 depicts the scanner system fully assembled in the protective glove bag environment.

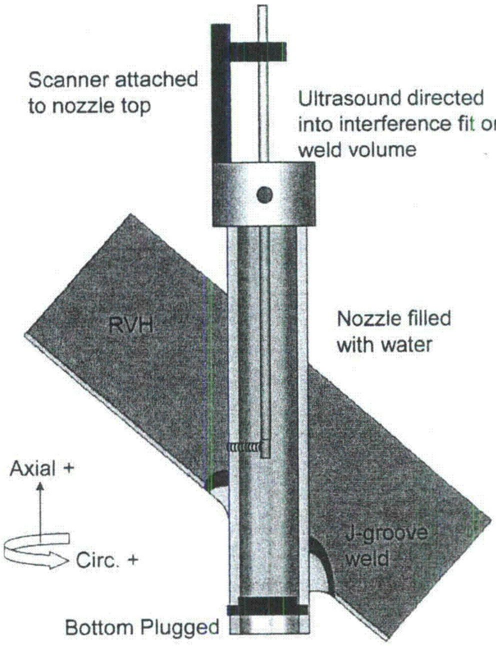

Figure 3.8 Scanning Setup/Orientation Schematic

Comment [PGO7]: Same as figure 5.3

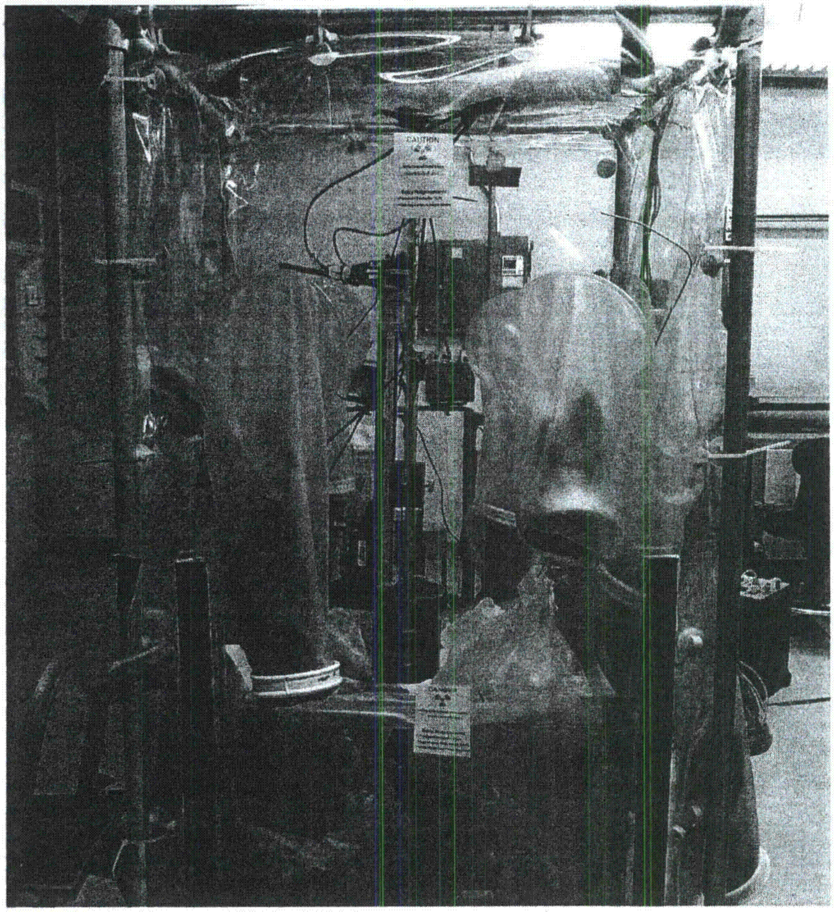

Figure 3.9 **Scanner System on Nozzle 63 in the Custom Glove Bag**

Comment [PGO8]: Same as figure 5.2.

4 Calibration Mockup

Prior to performing the non-destructive leak path assessment of Nozzle 63, a control rod drive mechanism (CRDM) mockup was constructed at Pacific Northwest National Laboratory (PNNL) for calibration of the ultrasonic testing equipment and to assess its capability to identify features associated with primary water leakage. These include crystalline boric acid in the interference fit region, wastage or corrosion of the low alloy steel reactor vessel head material, and cracking or degradation of the Alloy 600 nozzle material. A description of the mockup and testing is presented in this section.

4.1 Mockup Design and Fabrication

The CRDM mockup was made from an Alloy 600 tube fitted with two 6-in.-thick carbon steel blocks. The mockup was designed to simulate the interference fit between the CRDM nozzle and the reactor vessel head (RVH) material in a pressurized water reactor (PWR), using similar materials and fabrication techniques. The mockup had two interference fit regions as shown in Figure 4.1. In the top interference fit, notches were made in the tube and carbon steel blocks with electric discharge machining (EDM) to simulate cracking, wastage, and degradation of the materials. In the bottom interference fit, crystalline boric acid was placed between the tube and the carbon steel blocks to simulate deposits left by primary water leakage. Due to safety concerns (tipping) regarding specimen weight and center of mass, the flange end of the tube was bolted to a larger plate for increased stability.

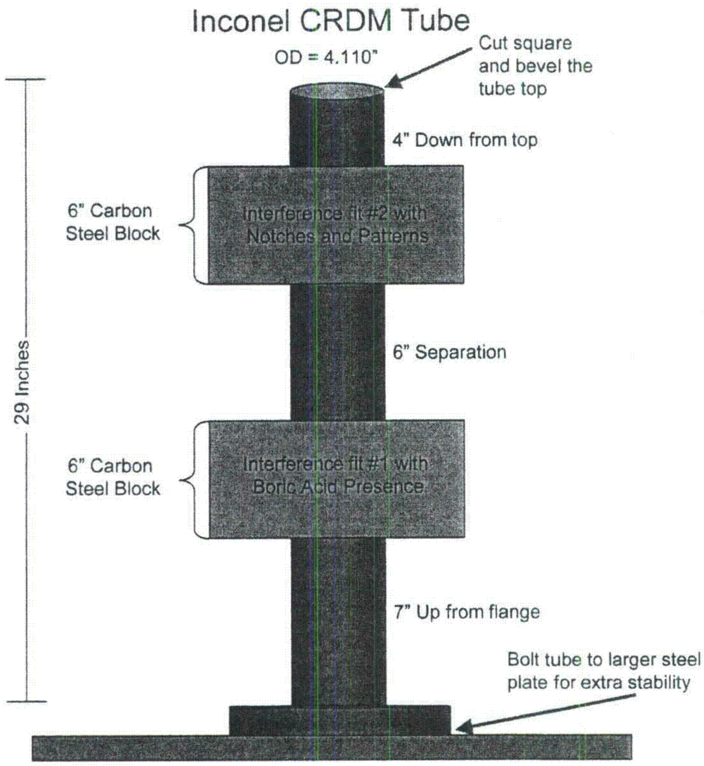

Figure 4.1 Assembled CRDM Interference Fit Mockup Specimen

4.1.1 Simulated Boric Acid Deposits

The lower interference fit on the CRDM nozzle mockup contained crystalline boric acid deposits in the region between the Alloy 600 tube and the carbon steel block. Boric acid deposits in the interference fit of an operating plant could indicate leakage of borated primary water through the J-groove seal weld. In-service-inspection data show that the presence of boric acid creates a unique ultrasonic transmission and reflection patterns in the fit regions (Cumblidge et al. 2009). The boric acid fit of the mockup was designed so that PNNL could evaluate and quantify this ultrasonic transmission and reflection phenomenon.

The lower interference fit mockup region was designed to have both regions where boric acid deposits were present and bare metal regions without boric acid, as shown in Figure 4.2. Ideally, the contrast of the two regions in the ultrasonic data would reveal differences in ultrasonic transmission and reflection. The process of creating the boric acid deposit regions began with masking off regions with tape on the Alloy 600 tube outer diameter (OD) where boric acid was unwanted, as shown in the left hand side of Figure 4.3. The boric acid was prepared for application by mixing a small amount of boric acid in solid form with a small amount of methanol. The two components were then sonicated into a paste with medium to high viscosity. The application of the acid involved spreading a thin and even coat of the paste with a compatible brush over the localized region on the OD of the tube between the masked-off sections. Upon evaporation of the methanol and solidification of the boric acid, the masking tape was removed. A snake-like pattern was scraped into one of the boric acid regions as indicated with the blue line in Figure 4.2 and the arrow in the right hand side of Figure 4.3.

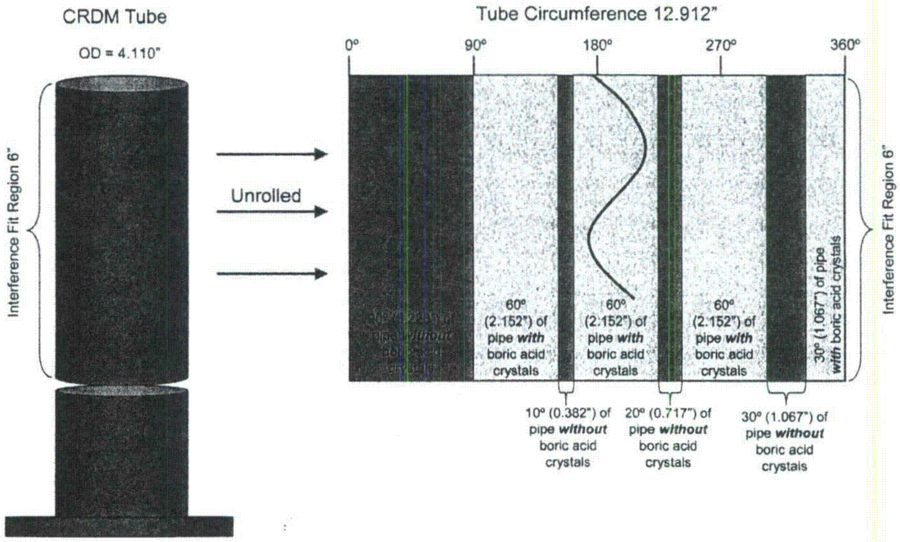

Figure 4.2 Boric Acid Pattern Conceptual Design

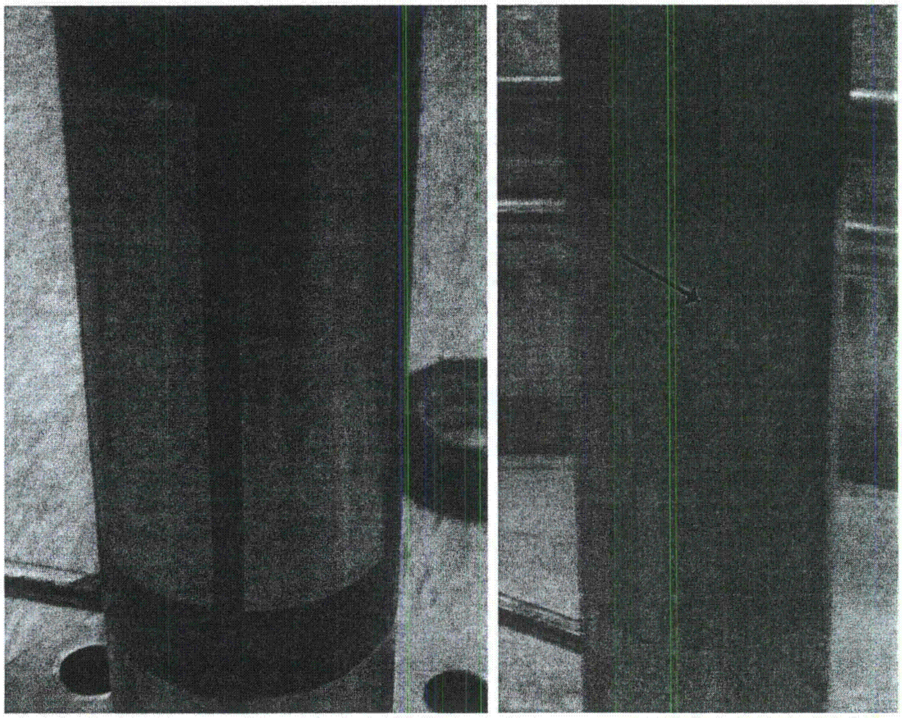

Figure 4.3 Boric Acid Application

Comment [PGO9]: State that in the image on the left the blue tape indicates masked regions and that the arrow on the right indicates the path where the boric acid was scraped off.

4.1.2 Simulated Cracking, Cutting and Wastage

The upper interference fit in the CRDM nozzle mockup contained various precision-crafted EDM notches to create a small void region between the tube and the carbon steel block. This was intended to simulate regions in the assembly where a void was created by wastage of the carbon steel RVH material or by anomalies in the CRDM tube such as machining marks, cracking, and steam cutting. The notches were machined by Western Professional, Inc., with the pattern shown in Figure 4.4, to provide ultrasonic detection limits and characterization information for voids in the interference fit region.

As shown in Figure 4.4, notches were put in both the Alloy 600 tube, which is the silver-colored region in the figure, and the carbon steel block, which is the brown/orange colored region. The tube and the carbon steel block had the same notch pattern, with the first 180 degrees of the mockup having the notches cut into the tube OD, and the area from 180 to 360 degrees having the notches cut into the carbon steel block inner diameter (ID). The notches were oriented horizontally and vertically to assess probe resolution in the circumferential and axial directions. A theoretically determined spot size using the 5-MHz phased-array probe at the interference fit region is 1.0 mm (0.04 in.) in both theta and Z directions (circumferential and axial directions).

For reference, the theoretical wavelength (λ) in the Alloy 600 tube material at 5 MHz is 1.1 mm (0.043 in.).

The probe resolution in both the circumferential and axial directions was measured by acquiring data on a series of notches 2-mm wide × 2-mm deep × 25-mm long (0.079-in. × 0.079-in. × 1.0-in.) that were spaced 2, 3, and 5 mm (0.079, 0.12, and 0.20 in.) apart (approximately 2, 3, and 5 λ), respectively. One set of these notches was orientated circumferentially and the other was oriented axially, as represented by blue lines in Figure 4.4. To measure width detection sensitivity, axial notches labeled 1–4 in Figure 4.4 were placed equidistant from each other and had a constant depth, while the widths varied from 0.7938 to 6.35 mm (0.03125 to 0.25 in.). The third set of notches was used to assess depth sensitivity, with axially oriented notches placed equidistant from each other. These notches are labeled 5–8 in Figure 4.4 and had constant lengths and widths but varied in depth. Figure 4.5 shows additional detailed notch dimensions. Complete as-built dimensional details for all of the notches can be found in Appendix A.

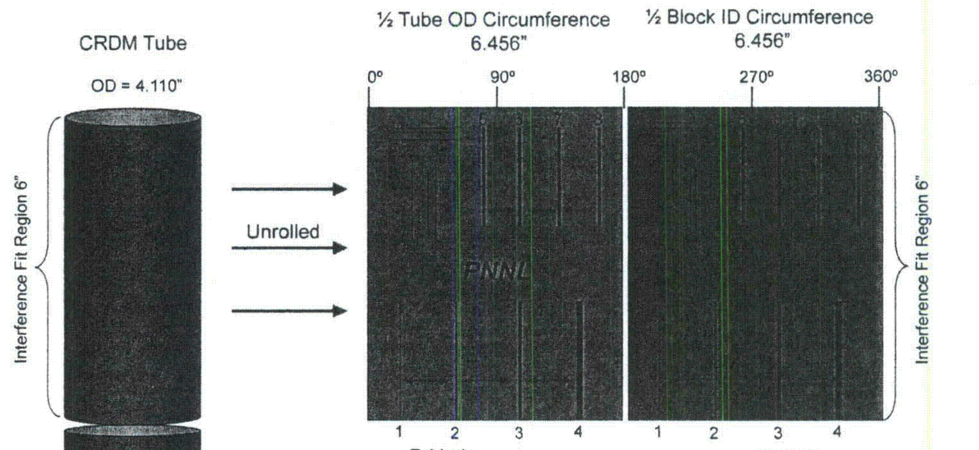

Table 1

Notch	Length (in)	Depth (in)	Width (in)
1	2.0	0.10	0.03125 (1/32)
2	2.0	0.10	0.0625 (1/16)
3	2.0	0.10	0.125 (1/8)
4	2.0	0.10	0.25 (1/4)

Table 2

Notch	Length (in)	Depth (in)	Width (in)
5	2.0	0.001	0.04 (1 mm)
6	2.0	0.002	0.04 (1 mm)
7	2.0	0.003	0.04 (1 mm)
8	2.0	0.005	0.04 (1 mm)

Figure 4.4 Interference Fit #2; Notch and Pattern Conceptual Design

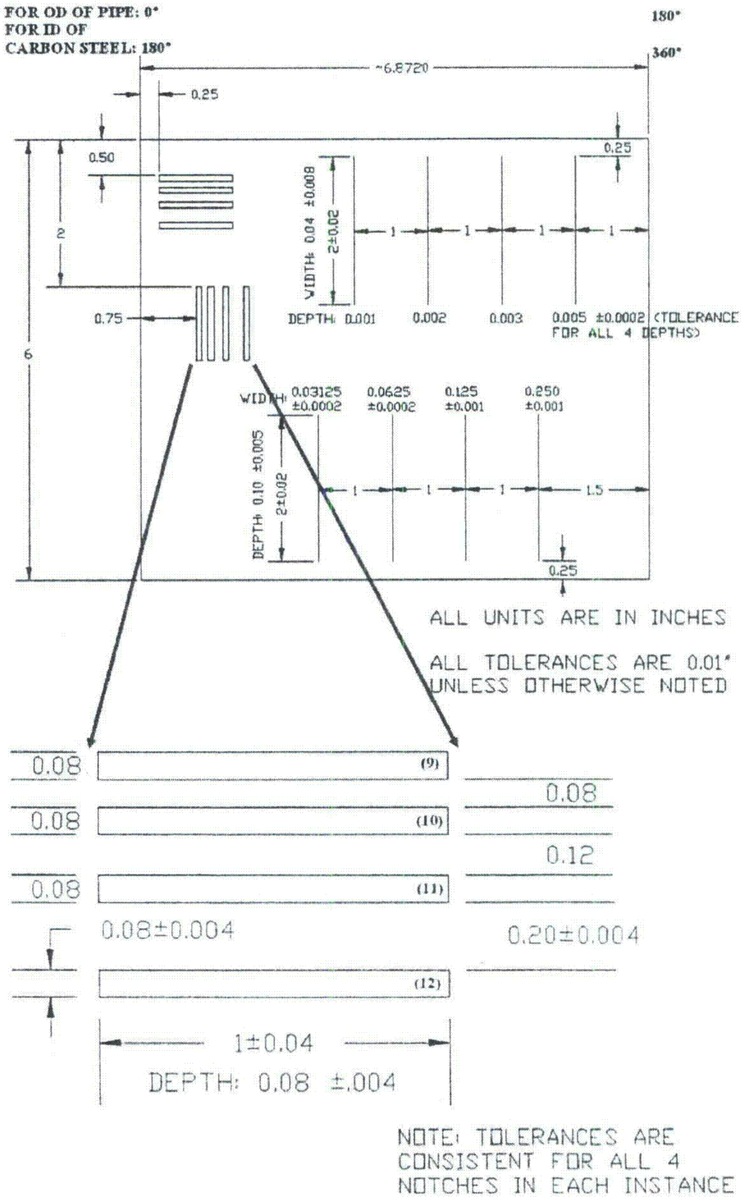

Figure 4.5 Notch Pattern in the CRDM Calibration Mockup Specimen, Upper Interference Fit. All units are inches. Above: General notch layout with detail. Below: Circumferentially orientated resolution notch detail.

Comment [PGO10]: Can this be in appendix? Do you need here?

The three sets or groupings of notches did not overlap, but were separated so that ultrasonic observations could be made independently on the ability to resolve two closely spaced indications, as well as width and depth sensitivity. The acronym 'PNNL' was also notched on the OD of the tube to provide an indication of off-axis sensitivity. Figures 4.6 and 4.7 show the EDM notch patterns as cut into the Alloy 600 tube and carbon steel block.

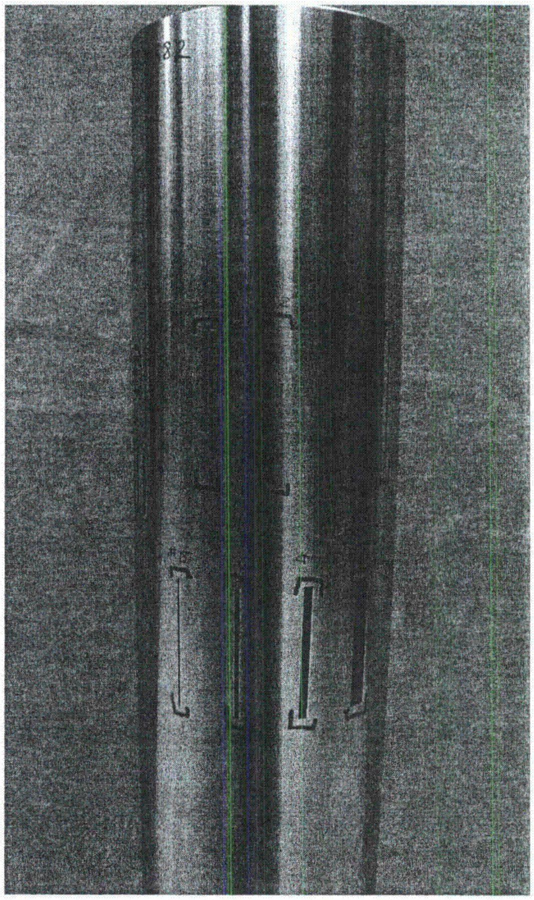

Figure 4.6 EDM Notches in Alloy 600 Tube

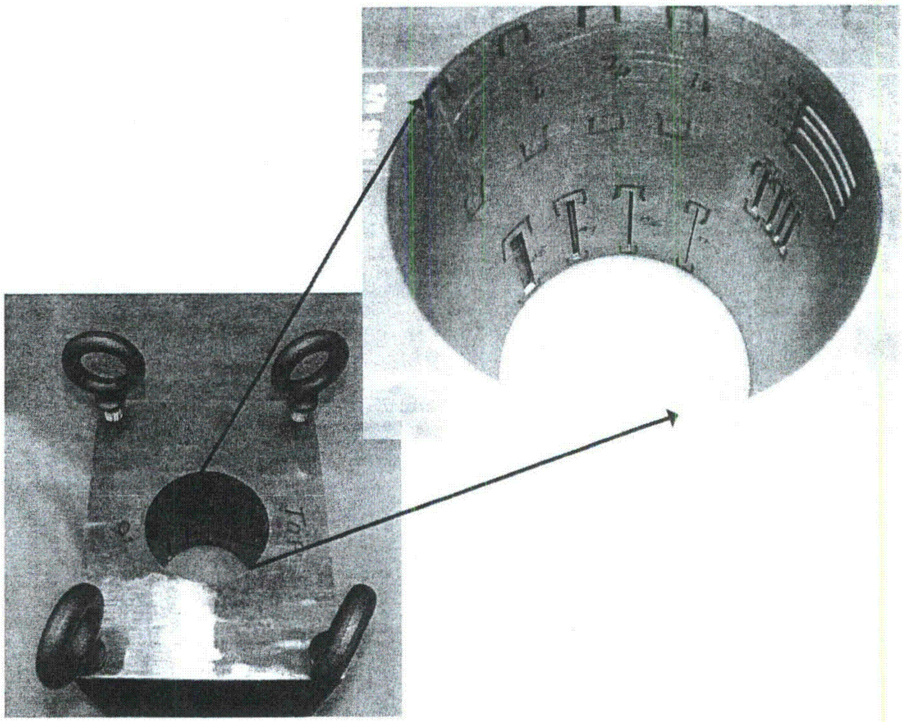

Figure 4.7 EDM Notches on Carbon Steel Block

4.1.3 Mockup Assembly

An interference fit is made by either heating the low alloy steel reactor pressure vessel (RPV) head or cooling the Alloy 600 nozzle, or both. PNNL choose to cool the nozzle. The other parameter considered was the size of the interference fit diameter. A suggested maximum fit was 0.102 mm (0.004 in.) (Gorman et al. 2009). Reported industry interference fit ranges were listed as 0.030 to 0.102 mm (0.0012 to 0.004 in.) (Hunt and Fleming 2002). PNNL decided to fabricate nominal 0.0762-mm (0.003-in.) interference fits.

The nozzle was lightly machined to remove any minor surface irregularities and its outer diameter was measured. Then the carbon steel blocks were machined with a hole that was 0.0762 mm (0.003 in.) in diameter smaller than the OD of the tube at room temperature of 22°C (72°F). The assembly of the CRDM mockup involved temporarily cold-shrinking the Alloy 600 tube with liquid nitrogen, so that it could be fitted with the carbon steel blocks. This created an interference fit of 0.0762 mm (0.003 in.) after all components returned to room temperature.

To determine if the interference fit was attainable, the expected thermal shrinkage for the nozzle at liquid nitrogen temperature was calculated. Thermal expansion coefficients are generally given in tabular form for different materials over a particular temperature range. These table values assume a linear relationship over a limited temperature range. Cryogenic material properties were needed for the temperatures used in forming the interference fit. Two reference papers (Clark 1968; Marquardt et al. 2002) discussed material properties of metal alloys at cryogenic temperatures. Inconel 718 was one of the materials studied and represented the nozzle material for the purpose of material shrinkage calculations. To form the interference fit, the nozzle was taken from room temperature, 293°K (19.85°C, 67.73°F), to the temperature of liquid nitrogen, 77.2°K (−195.95°C, −320.71°F). Clark (1968) measured the thermal expansion coefficients from liquid hydrogen temperature to room temperature, 20°K (−253.15°C, −423.67°F) to 293°K (19.85°C, 67.73°F), in 10- or 20-degree steps for different metallic alloys. Results were presented in tabular form for the expansion or shrinkage relative to room temperature. From the table for Inconel 718 at 80°K:

$$223 = \left[(L_{293} - L80) / L_{293}\right] \times 10^5 \tag{4.1}$$

expansion relative to room temperature

where L_n = length at temperature n, in degrees K.

From Eq. (4.1), the shrinkage of the 104.14-mm (4.1-in.) diameter Alloy 600 tube at liquid nitrogen temperature relative to room temperature is calculated as approximately 0.232 mm (0.00914 in.).

Marquardt modeled the material properties over a large temperature range (4 to 300°K [−452.5 to 80.3°F or −269.2 to 26.9°C]) with a polynomial or a logarithmic polynomial equation. An equation for the integrated linear thermal expansion or shrinkage is given as:

$$\left(L_T - L_{293}\right)/L_{293} = \left(a + bT + cT^2 + dT^3 + eT^4\right) \times 10^{-5} \tag{4.2}$$

The coefficients for 718 Inconel are listed as:

a = −2.366E+02
b = −2.218E-01
c = 5.601E-03
d = −7.164E-06
e = 0

From Eq. (4.2), the shrinkage of the tube is calculated as approximately 0.233 mm (0.00917 in.) at 77K. This result very closely matches the result from Eq. (4.1) given above.

Prior to assembly of the mockup, experimental verification of the calculated shrinkage was conducted on a section of Alloy 600 tubing cut from a tube similar to that which was used for the mockup. At room temperature, five outside diameter measurements were acquired at 0–180 and five at 90–270 degrees using a calibrated caliper, shown in Figure 4.8, at marked locations along the axial length of the specimen. Temperature measurements were obtained using a Raytek ST80XXUS infrared (IR) standoff thermometer. At room temperature the average diameter of the tube was 104.902 mm (4.130 in.). The tube section was then submerged in a liquid nitrogen (LN) bath for approximately 2.5 minutes. The chilled tube section was promptly removed from the LN bath and the diameter of the tube was again measured at the same locations. The temperature of the tube upon removal from the LN bath was unattainable as it surpassed the low end capability of the IR thermometer (−32 to 760 degrees C [−25 to 1400 degrees F]). The theoretical temperature of LN is −195.95 degrees C (−320.71 degrees F). At cold temperatures, the average diameter of the tube was 104.699 mm (4.122 in.). The tube section was allowed to re-equilibrate to room temperature and additional diameter measurements were made. These showed that the average nozzle diameter returned to 104.902 mm (4.130 in.). A full set of diameter data can be viewed in Table 4.1, where data were acquired in descending order from position 5 to 1. Figure 4.9 shows the tube diameter at the three stages of this experiment as a function of axial position: room temperature initial (RT initial), after LN, and room temperature final (RT final). The results from this test indicated that the Alloy 600 tube material shrank an average of 0.203 mm (8 mils) in diameter when chilled with LN and then was restored to its original size after returning to room temperature. The CRDM calibration specimens were designed and machined for a 0.076-mm (3-mils) diameter interference fit. Tube shrinkage of an additional 0.127 mm (5 mils) provided the necessary room for slipping the machined carbon steel blocks over the tube during mockup assembly. Moreover, it was equally important that the tube return to its original size (at room temperature) in order to create the tight interference fit. This successful preliminary test proved that both necessary requirements could be achieved.

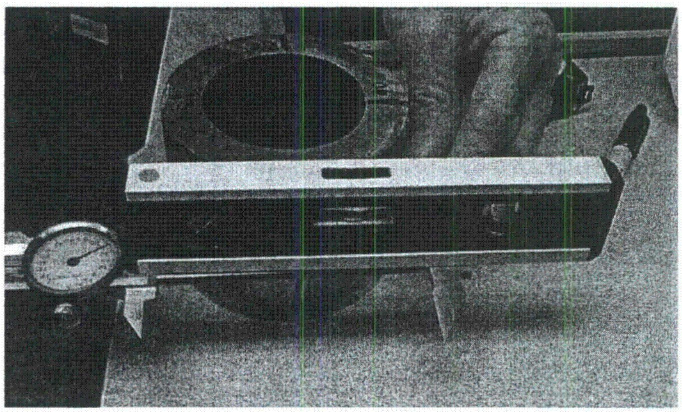

Figure 4.8 Diameter Measurements Acquired at Room Temperature Using a Caliper

Table 4.1 Alloy 600 Tube Diameter Measurements Verses Temperature

		Room Temp		Liquid Nitrogen			Return to Room Temp	
Temp (F)		73.9		Unknown			73.9	
Diameter (in.)		0–180	90–270	0–180	90–270		0–180	90–270
	1	4.130	4.130	4.122	4.125		4.130	4.130
	2	4.130	4.130	4.122	4.122		4.130	4.130
	3	4.130	4.130	4.124	4.122		4.130	4.130
	4	4.130	4.130	4.120	4.122	Λ	4.130	4.129
	5	4.130	4.130	4.120	4.122	t=0	4.130	4.129
Average:		4.130		4.122			4.130	

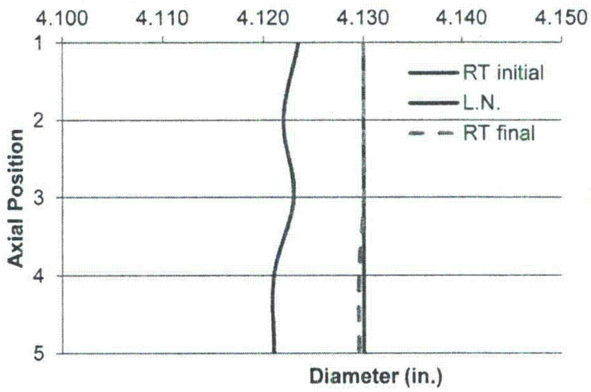

Figure 4.9 Tube Shrinkage Measurements

Comment [PGO11]: This extended discussion isn't necessary.

To assemble the mockup, LN was used to shrink the 736.6-mm (29-in.) long Alloy 600 tube. As the tube rested vertically in a stainless steel secondary containment trough, LN was added in the tube to within 101.6 mm (4 in.) below the top, as shown in Figure 4.10. The LN was contained solely within the tube. A permanent end cap was seal welded at the flange end of the tube to prevent leakage of any LN. Towels were used to assist in insulating the tube to prevent unwanted heat transfer and/or ice formation on the OD of the tube. Once the tube cavity was full of LN, the OD of the tube was monitored until the maximum shrinkage level was achieved. As measured at the top of the tube, a diameter-shrinkage of 8 mils (0.20 mm) was achieved.

Comment [PGO12]: Global comment: please make sure metric units (English in parens.)

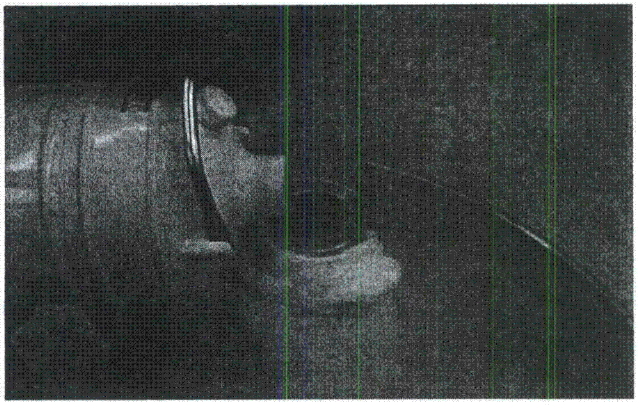

Figure 4.10 Filling Alloy 600 Tube with Liquid Nitrogen

The first fit to be made was the lower one with simulated boric acid deposits. Oversized polyvinyl chloride (PVC) piping was cut to length and fitted over the Alloy 600 tube and served as a hard stop for the carbon steel block to rest on while the specimen returned to room temperature, as seen in Figure 4.11. Next, the insulation towels were removed and the machined carbon steel block was hoisted over top of the tube and aligned accordingly. The block was lowered rapidly and slid down the Alloy 600 tube, but came to rest approximately 63.5 mm (2.5 in.) above the targeted resting place. Thus, the boric acid deposits were only under the bottom half of the carbon-steel block. Upon return to room temperature, the PVC piping was no longer needed and was removed.

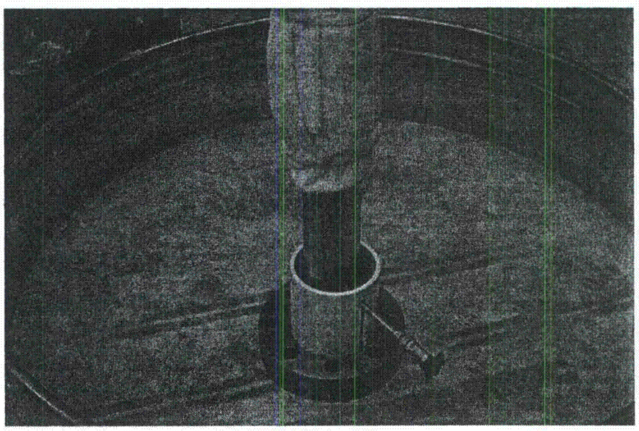

Figure 4.11 PVC Spacer Shown at Bottom of Specimen

The second interference fit with machined notches was created following a similar protocol. For this fit, it was critical to align the zero degree point of the carbon steel block with the zero degree point stamped on the Alloy 600 tube so as to not overlap the notch patterns created in the two materials. The assembly of this fit went according to plan using the PVC piping separator during assembly to maintain separation between the two fit regions. Figure 4.12 shows the completed and assembled calibration specimen.

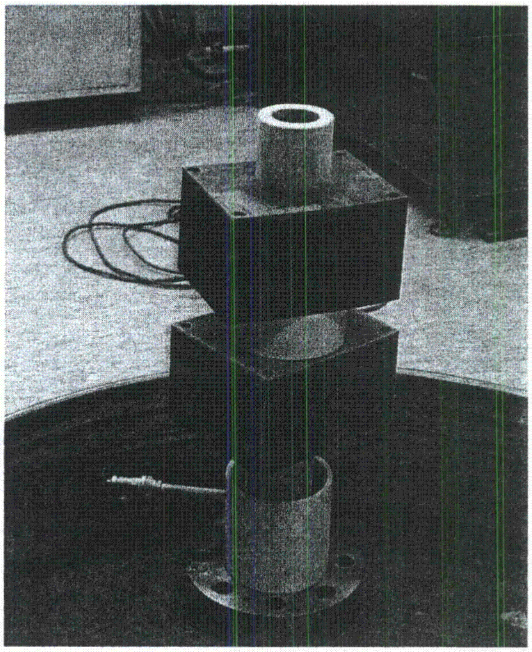

Figure 4.12 Assembled Calibration Specimen

4.2 Ultrasonic Evaluation of Mockup

The CRDM nozzle mockup was examined with the annular ultrasonic phased-array probe described in Section 2. The results of the mockup examination are presented in the following sections.

4.2.1 Alloy 600 Tube Notches

The machined notches in the Alloy 600 tube of the CRDM nozzle mockup simulated potential cracks or degradation of the nozzle penetration. The notched area shown in Figures 4.4 and 4.5 was scanned over approximately a 0 to 170 degree range in the circumferential direction (horizontal axis) and 0 to 180 mm (7.1 in.) in the axial direction (vertical axis) with the data image shown in Figure 4.13. This top view, plan view, or C-scan image shows the resolution notches in the upper-left portion of the image. The variable depth and width notches are also seen as well as the letters "PNNL." The color scale is displayed on the left with lowest amplitudes at the bottom represented by white and the highest amplitude at the top of the color bar represented by red. In this pulse-echo data, the low amplitude signals (blue and green) indicate good transmission or low reflection of the ultrasonic energy at the interface of the tube to the carbon steel. Conversely, the high-amplitude signals (yellow and red) represent poor transmission or large reflection at the interface. A large reflected signal would be generated at a tube-to-air interface as would be seen above and below the interference fit region or in the presence of a notch with large enough dimensions.

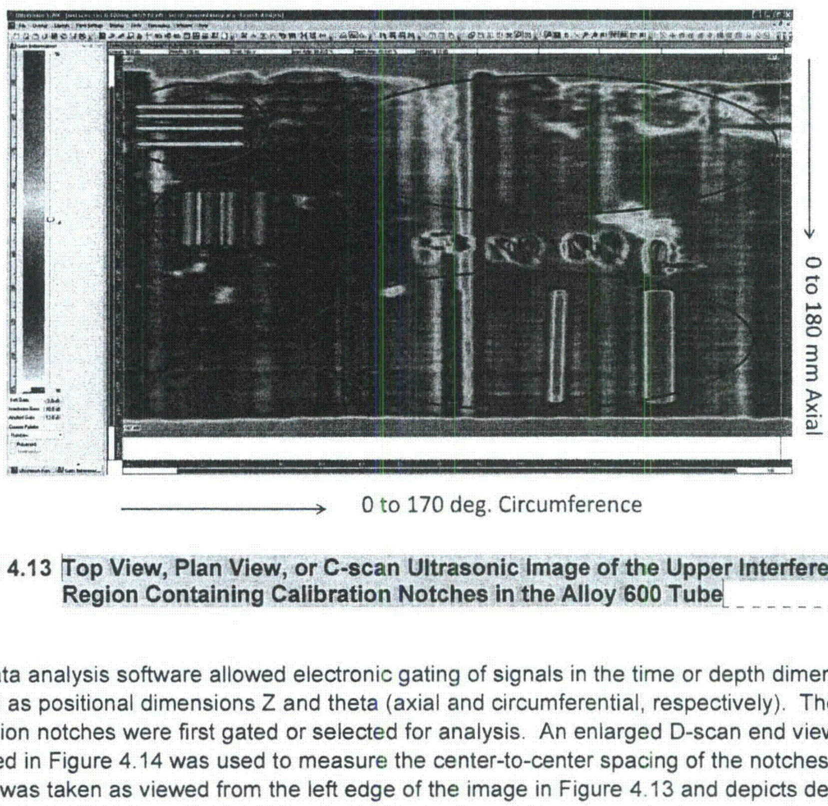

Figure 4.13 Top View, Plan View, or C-scan Ultrasonic Image of the Upper Interference Fit Region Containing Calibration Notches in the Alloy 600 Tube

Comment [PGO13]: Please state in the figure caption what is circled

The data analysis software allowed electronic gating of signals in the time or depth dimension as well as positional dimensions Z and theta (axial and circumferential, respectively). The axial resolution notches were first gated or selected for analysis. An enlarged D-scan end view, as depicted in Figure 4.14 was used to measure the center-to-center spacing of the notches. This image was taken as viewed from the left edge of the image in Figure 4.13 and depicts depth into the material (along the sound path) in the vertical axis and the scanner index or nozzle axial direction in the horizontal axis. From this end view, an "echodynamic" curve or profile was generated along the red horizontal line drawn through the responses from the notches, and was plotted above the image. The measured notch widths, from left to right, as measured at the half-amplitude points, were 2.0, 2.0, 2.5, and 2.5 mm (0.08, 0.08, 0.10, and 0.10 in.), respectively. This represents only 4 or 5 pixels with each pixel equal to 0.5 mm (0.02 in.). The actual notch widths were 2.08, 2.06, 2.16, and 2.11 mm (0.082, 0.081, 0.085, and 0.083 in.), respectively. Notch depths were measured as 2.06, 2.06, 2.03, and 2.03 mm (0.081, 0.081, 0.080, and 0.080 in.), respectively. Actual depths were 2.06, 1.95, 2.00, and 2.00 mm (0.081, 0.077, 0.079, and 0.079 in.), respectively. The data suggested that cracks as small as approximately 1 mm (0.04 in.) in depth could be accurately measured. Also, the notches could be clearly distinguished from each other, providing an indication of lateral probe resolution in the nozzle axial direction. In this set of notches, the actual center-to-center separations were 7.11, 5.08, and 4.06 mm (0.28, 0.20, and 0.16 in.), respectively. The measurements from the ultrasonic data gave separations of 7.0, 5.5, and 4.0 mm (0.28, 0.22, and 0.16 in.), respectively. These highly correlated data values and the data image indicated that an axial resolution of better than 4.0-mm (0.16-in.) was achievable.

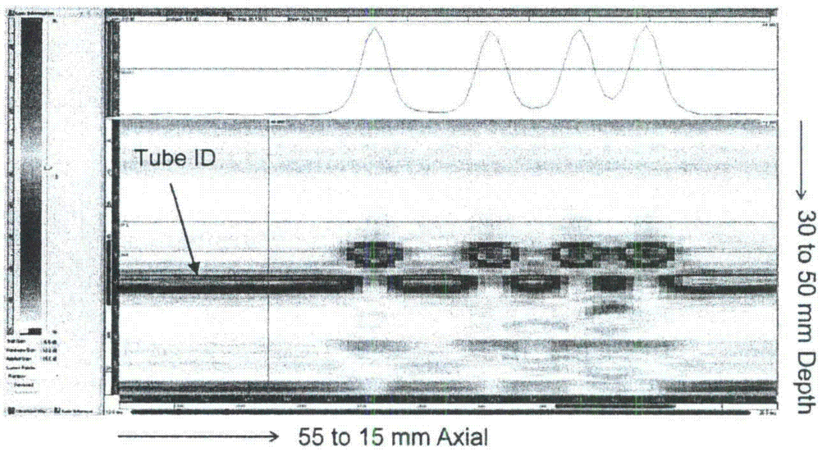

Figure 4.14 D-scan End View of the Axial Resolution Notches in the Inconel Tube

The gated circumferential resolution notch set is shown in Figure 4.15. This image was taken as viewed from the bottom edge in Figure 4.13. Notice that the closely spaced two notches on the left are overlapping but they are still resolvable. Peak-to-peak values gave measured notch separations of 4.36, 5.18, and 6.82 mm (0.17, 0.20, and 0.27 in.), respectively. The actual separations were 4.06, 5.08, and 7.11 mm (0.16, 0.20, and 0.28 in.), respectively. This is greater error than was observed for the axial direction. This test demonstrated a circumferential probe resolution of approximately 4.4 mm (0.17 in.).

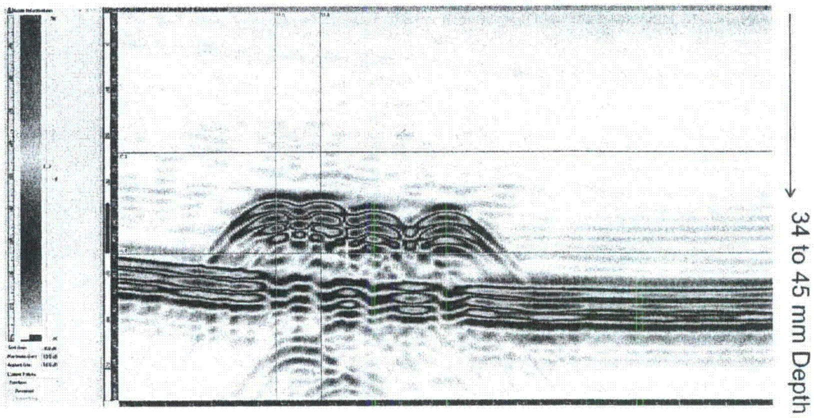

Figure 4.15 B-scan Side View of the Circumferential Resolution Notches in the Inconel Tube

The set of notches in the upper right portion of the scanned image in Figure 4.13 varied in depth but had constant width. These very shallow notches were recognized because their shape and location were known, but they could have been missed based on amplitude response alone. Machining marks on the tube as well as variations in the interference fit produced a non-uniform background response for the fit region, complicating the detection. The center-to-center separations of these notches as ultrasonically measured were 23.84, 24.29, and 23.61 mm (0.939, 0.956, and 0.930 in.), respectively, whereas the actual spacing was 25.4 mm (1.0 in.) between each notch. Flaw depth information was not discernable in the first interference fit echo, but the second echo gave some indication of a flaw tip as noted by the red arrows in the upper part of Figure 4.16. This image represents the B-scan side view of the data while the lower image is a C-scan top view. A higher inspection frequency could have better resolved the small depth variations in these notches. The current second-echo ultrasonic data showed an approximate depth of 0.15 mm (0.006 in.) for all four notches, whereas the actual depths were 0.028, 0.051, 0.76, and 0.13 mm (0.001, 0.002, 0.003, and 0.005 in.), respectively. While these very shallow notches each presented a discontinuity that was ultrasonically detected, their depths were below the system depth or range resolution. For a greater than 50% bandwidth probe, the range resolution is on the order of one wavelength, which in Alloy 600 is approximately 1.1 mm (0.043 in.) at a 5-MHz inspection frequency.

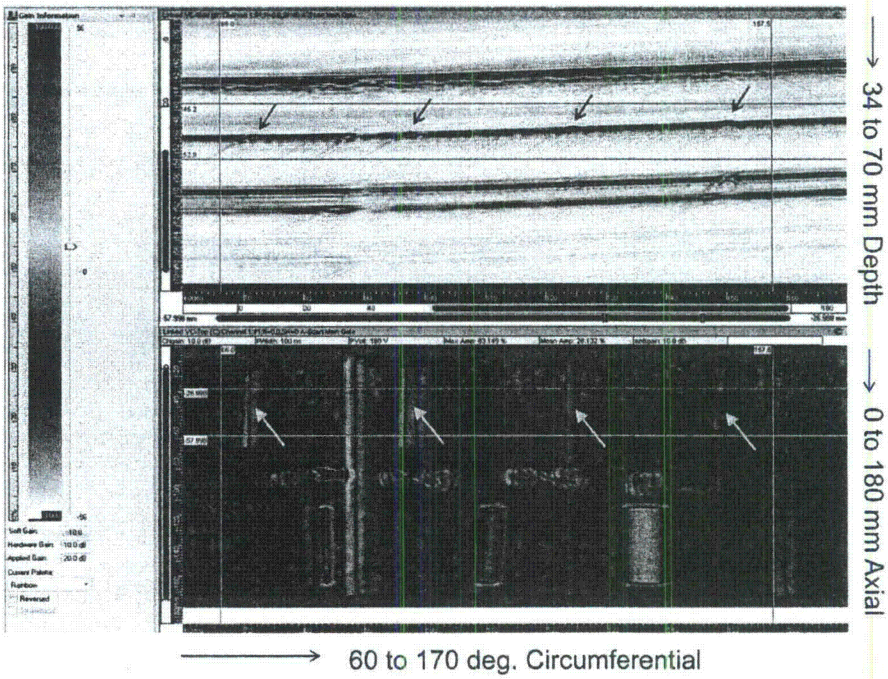

Figure 4.16 The Second Echo is Gated in the Side View Image in the Top of Figure with the Horizontal Lines. The corresponding C-scan top view is displayed in the bottom image. This second echo captures a disturbance in the back-wall echo showing some depth information, noted by the red arrows at top.

Comment [PGO14]: State what arrows are pointing to in bottom image.

The final set of notches contained width variations and are shown in Figure 4.17. These flaws were ultrasonically measured with depths of 2.2, 2.5, 2.7, and 2.9 mm (0.09, 0.10, 0.11, and 0.11 in.), respectively, left to right in the image, while the actual depth was 2.53 mm (0.10 in.) for all notches. The measured center-to-center spacings were 23.1, 24.8, and 23.8 mm (0.91, 0.98, and 0.94 in.), respectively, while actual spacings were all 24.5 mm (1.00 in.). Finally, the widths of the flaws were measured in two ways. The first method used the width of the upper part of the flaw response, and the second method used the width of the loss of back-wall signal. The loss of back-wall signal technique was more accurate with measured widths of 3.91, 3.36, 5.00, and 8.82 mm (0.099, 0.126, 0.154, and 0.298 in.), respectively. Actual widths were 0.80, 1.61, 3.24, and 6.42 mm (0.031, 0.063, 0.127, and 0.253 in.), respectively. When measured from the second ultrasonic back-wall echo, the loss of signal measurements gave notch widths of 1.36, 2.73, 3.82, and 7.00 mm (0.054, 0.107, 0.150, and 0.276 in.), which were closer to the actual values. The probe spot size when focused at the interference fit, or 15 mm (0.59 in.) into the Alloy 600, was modeled at 1.2 $\times$1.2 mm (0.047 $\times$ 0.047 in.) at the –6 dB points. Flaw width sizing values are typically oversized by the probe spot size so these measured width values were well within the error expected with this probe.

In summary, the system resolution for defects as represented by notches in the Alloy 600 tube was better than 4 mm (0.16 in.) in the axial direction and 4.4 mm (0.17 in.) or greater in the circumferential direction. The depth or range resolution notches, as small as 0.028 mm (0.0011 in.), were beyond the system limits for depth sizing but the notches were detected. Range resolution was estimated at 1 mm (0.039 in.). Notches as narrow as 0.80 mm (0.031 in.) in the circumferential direction were detected and sized but the limits were somewhat dependent on the machining marks and other anomalies in the materials and interference fit that also gave ultrasonic indications.

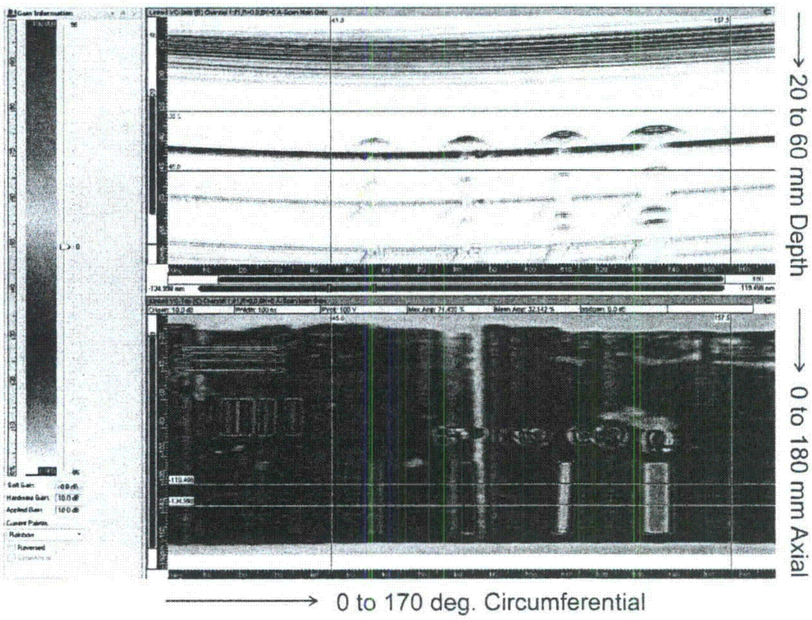

Figure 4.17 B-scan Side View on Top and C-scan Plan View on Bottom of the Width Varying Notches in the Inconel Tube

4.2.2 Carbon Steel Notches

The 180–360 degree portion of the upper fit region in the CRDM mockup contained notches in the carbon steel block to simulate degradation or wastage of the RPV head material. These notches were on the far side of the interference fit relative to the location of the probe. Because the interference fit was not uniform, the notch responses were not as clear as those for notches in the tube, as evident in Figure 4.18.

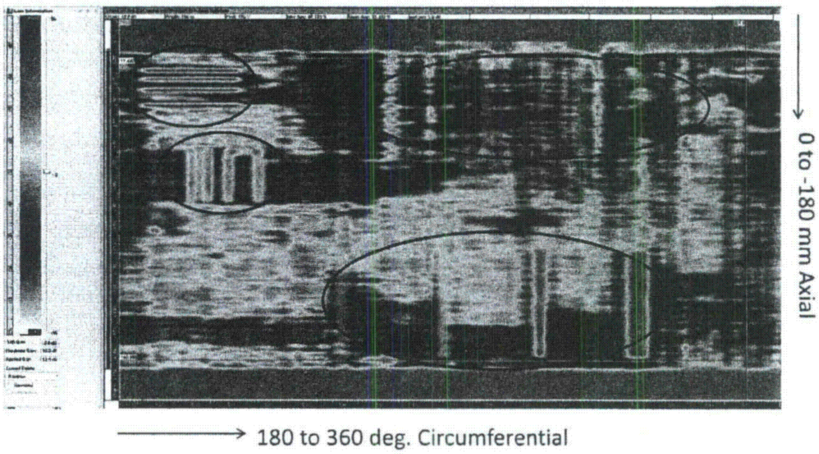

Figure 4.18 **C-scan Plan View of the Notches in the Carbon Steel from the First Ultrasonic Echo**

Comment [PGO15]: State what is circled.

The axial resolution notches in the top left of the figure were resolved, but the lower notch was on the edge of a high-amplitude region. The measured center-to-center spacings were 3.90, 4.58, and 6.88 mm (0.15, 0.18, and 0.27 in.), respectively, while actual spacings were 4.06, 5.08, and 7.11 mm (0.16, 0.20, and 0.28 in.), respectively. Axial resolution was therefore approximately 4 mm (0.16 in.) or better.

Measurements from the circumferential resolution notch pattern showed center-to-center spacings of 3.82, 5.00, and 7.54 mm (0.15, 0.20, and 0.30 in.), respectively, with actual spacings of 4.06, 5.08, and 7.11 mm (0.16, 0.20, and 0.28 in.). Circumferential resolution was also approximately 4 mm (0.16 in.) or better.

The variable depth notches in the top right of Figure 4.18 were detected but depths could not be measured. First and second echo images are shown in Figures 4.19 and 4.20, respectively. Center-to-center spacing was ultrasonically measured at 23.9, 22.4, and 24.4 mm (0.94, 0.88, and 0.96 in.), respectively, with an actual spacing of 25.4 mm (1.00 in.) for all notches.

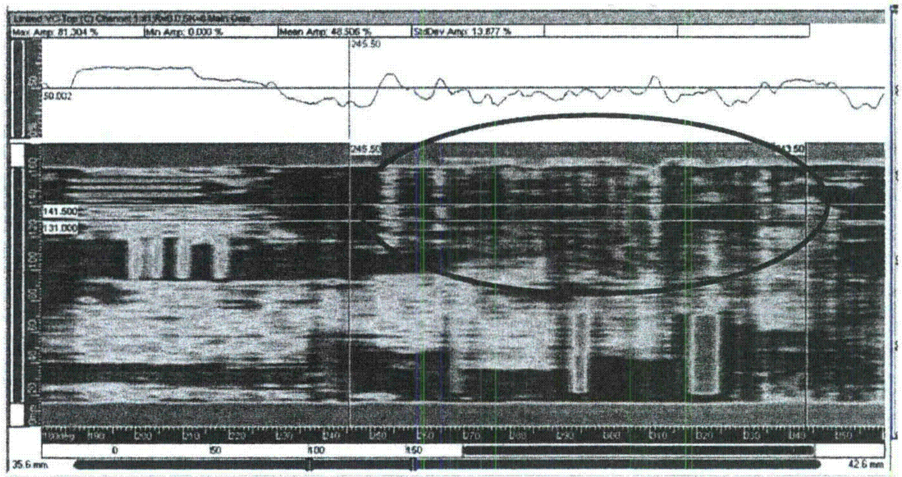

Figure 4.19 C-scan Plan View of the Depth Notches in Carbon Steel, on the Upper Right. This image was acquired from the first ultrasonic echo.

Comment [PG016]: Say what is circled.

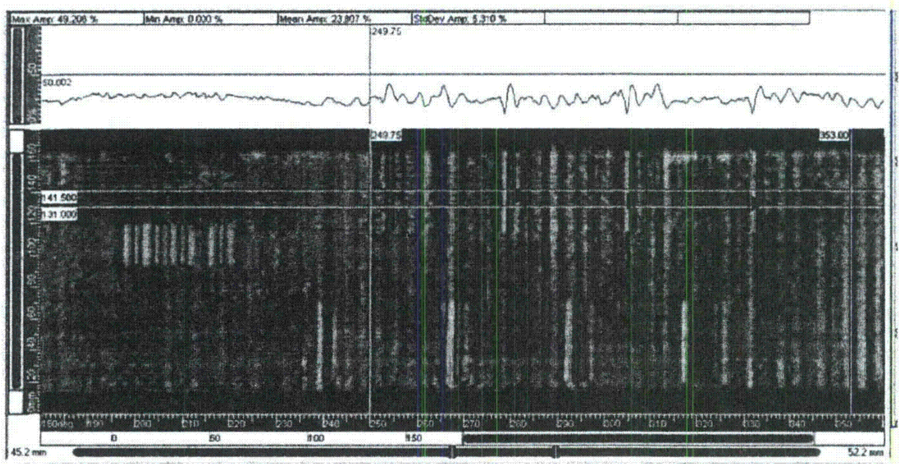

Figure 4.20 C-scan Plan View of the Depth Notches in Carbon Steel, on the Upper Right. This image was acquired from the second ultrasonic echo.

Comment [PG017]: Say what arrows are pointing to.

The set of notches with variable widths is shown in Figure 4.21 with the notches marked by red arrows at the bottom of the image. This image represents the second echo. The center-to-center spacing measurements were 25.4, 23.2, and 25.0 mm (1.00, 0.91, and 0.98 in.), respectively, left to right, with actual spacing of 25.4 mm (1.00 in.). Measured notch width values were 1.82, 2.27, 4.27, and 6.82 mm (0.072, 0.089, 0.168, and 0.268 in.), respectively, with actual values of 0.80, 1.59, 3.18, and 6.39 mm (0.032, 0.062, 0.13, and 0.25 in.), respectively. The notch widths were also measured from the first echo (refer to Figure 4.18, a first ultrasonic echo image) with slightly poorer results.

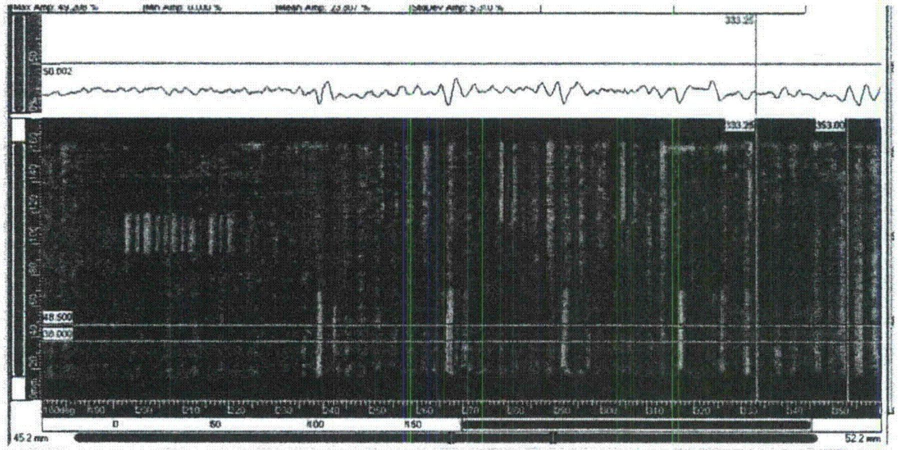

Figure 4.21 C-scan Plan View of the Width Notches in Carbon Steel, on the Bottom. This image was acquired from the second ultrasonic echo.

Comment [PGO18]: Say what arrows are pointing to.

In summary, the system resolution for defects as represented by notches in the carbon steel was better than 4 mm (0.16 in.) in both the axial and circumferential directions. The depth or range resolution notches, as small as 0.028 mm (0.0011 in.), were beyond the system limits for sizing but the notches were detected. In general, the notch depth into the carbon steel is not measureable because the sound beam is reflected at the first tube-to-air interface and does not travel through the air gap to the back of the cavity in the steel. Notches as narrow as 0.80 mm (0.10 in.) in the circumferential direction were detected.

4.2.3 Simulated Boric Acid Deposits

The top view, C-scan images from the mockup with boric acid deposits in the interference fit region are displayed in Figures 4.22 and 4.23. The first image represents the 60 to 240 degree circumferential region and the second image represents the 240 to 60 degree circumferential region, both as captured by the first echo. The boric acid regions were readily detected as lower amplitude response and are outlined with red boxes. Again, notice machining marks and non-uniformity in the interference fit response. The amplitude relevance is discussed in the next section.

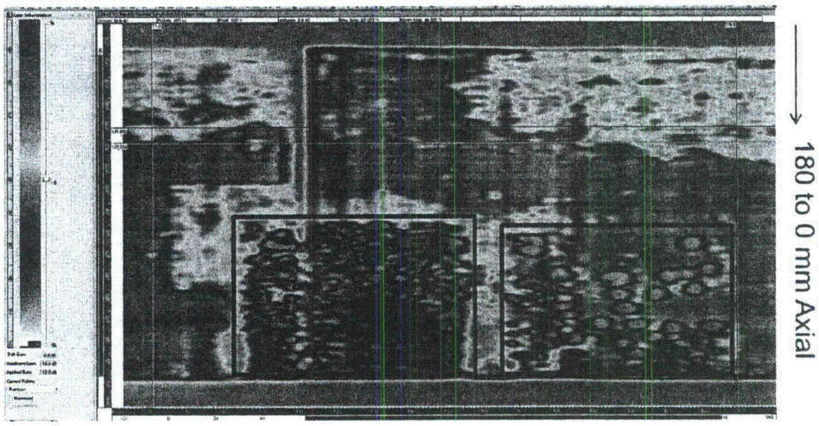

Figure 4.22 **C-scan Plan View of the Boric Acid Deposits in the Lower Interference Fit Region. The horizontal axis represents the circumferential range of 60–240 degrees. This image is from the first ultrasonic echo.**

Comment [PGO19]: Say what is boxed.

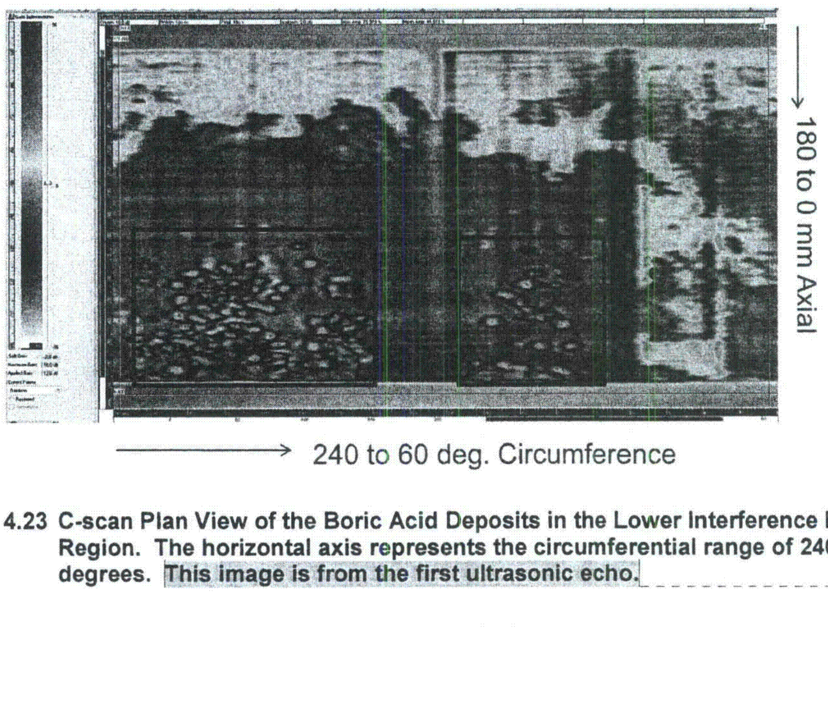

Figure 4.23 **C-scan Plan View of the Boric Acid Deposits in the Lower Interference Fit Region. The horizontal axis represents the circumferential range of 240–60 degrees. This image is from the first ultrasonic echo.**

Comment [PGO20]: Say what is boxed.

4.2.4 Amplitude Response

In addition to characterizing the notch response data for probe spatial and range resolution and flaw detection capability, an analysis of the acoustic response from the different regions was performed based on the reflected signal strength in the lower boric acid mockup section. The three categories represented in the data were the interference fit region where no boric acid was present, the interference fit region where boric acid was present, and the tube region outside of the interference fit area. These areas are represented in Figure 4.24 for the 60 to 240 degree boric acid image. The portion of the image outlined with the red box represents the interference fit region where boric acid deposits were present, the black dashed boxes represent the tube regions above and below the interference fit, and the black dotted boxes represent regions in the interference fit without boric acid deposits. The mean and peak amplitudes were measured in each of these boxed areas from the C-scan image. Similar measurements were also acquired for the 240 to 60 degree boric acid image.

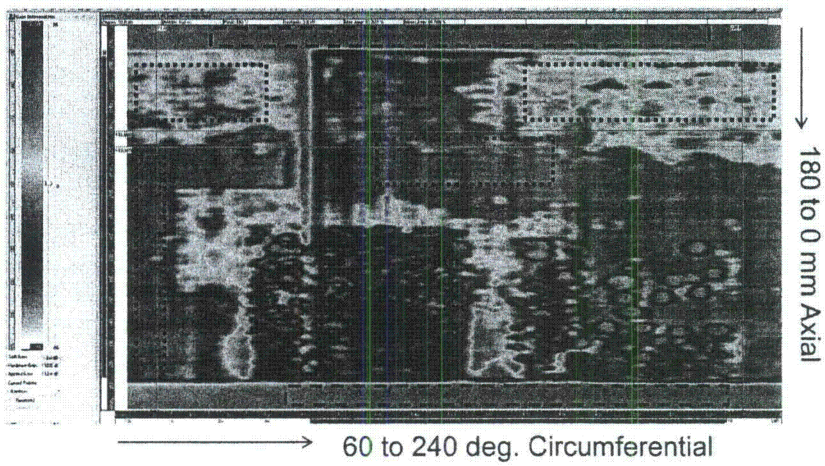

Figure 4.24 The Interference Fit Region Containing Boric Acid is Subdivided into Three Regions. The red box represents the presence of boric acid in the interference fit region, the black dashed boxes represent the tube region, and the black dotted boxes represent the interference fit region.

The data images were analyzed with a total image gain of 12 dB. This represented 10 dB of hard gain applied during acquisition and 2 dB of soft gain applied during analysis. The mean responses from the interference fit regions without boric acid deposits were in the range of 40 to 55 percent of full-screen amplitude. This range of values was due to the variability in the fit itself. Some regions of the fit were tight, giving lower reflected amplitude and more transmitted energy. This condition is represented by the green color in the image. Other regions of the fit showed higher reflected energy (not tight), thus less transmitted energy, and this state is represented by the yellow-to-orange colors. Machining marks were evident and also lead to response variability. The mean responses of the interference fit regions with boric acid deposits were in the range of 24 to 30 percent range of full-screen height (FSH). This shows more energy transmitted (less reflected) through the interference fit region with the presence of boric acid than in the regions without boric acid. The boric acid crystals filled gaps in the fit and efficiently coupled the ultrasonic energy into the carbon steel material. Finally, the mean responses of the tube regions above or below the interference fit were 60 to 75 percent of FSH, demonstrating greater reflectance of energy at the outside tube surface-to-air interface. These measurements established a baseline for the Alloy 600 tube-to-air interface reflectivity level. It also indicated that orange-colored regions in the interference fit represented an air gap. These mockup data images showed that interference fit region where no boric acid is present, the interference fit region where boric acid is present, and the tube region above or below the interference fit area are distinguishable by their mean ultrasonic response.

A final study was conducted as a result of discussions with John P. Lareau of WesDyne International on industry-style CRDM inspections and practices. He reported that the presence of boric acid was simulated with clay on a nozzle mockup specimen and gives an ultrasonic response that is 2 dB lower than the nozzle without clay. To evaluate the PNNL inspection system under a similar scenario, putty was placed on the outside of a blank nozzle specimen. The results are displayed in Figure 4.25 and clearly show that the system detects the putty as displayed by the yellow flower and butterfly characters in the C-scan image. The mean response from the putty region was measured at 64.8 percent of FSH and the clean nozzle response was 72.0 percent. This represents a 0.9 dB drop in amplitude. This smaller response difference is possibly due to the type of clay used in the WesDyne testing as compared to the putty used at PNNL.

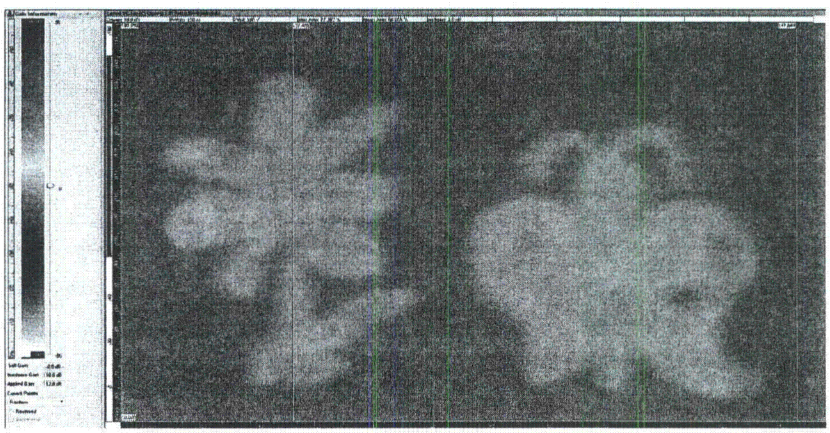

Figure 4.25 **Putty on a Nozzle Outer Surface is Detected. The horizontal axis represents 250 mm (9.8 in.) and the vertical axis represents 90 mm (3.5 in.).**

Comment [PGO21]: Please don't show this figure. It is distracting. Do you have an image with different shapes or can we describe with words only.

5 Nozzle 63 Nondestructive Leak Path Assessment

After calibration and testing on the control rod drive mechanism (CRDM) mockup, the phased array ultrasonic equipment was transported to the Radiochemical Processing Laboratory (RPL/33) for the examination of Nozzle 63. The results of the examination are presented in this section.

5.1 Scanner Setup

A CRDM nozzle was used to assess the functionality of the probe, scanner, and electronics after they were moved to RPL/33 where Nozzle 63 was housed. A simple scan on the nozzle was performed in the ultrasonic laboratory where the mockup was tested and then in RPL/33 after transporting and reassembling all of the equipment. Data images before and after transport are displayed in Figure 5.1. These images represent C-scan top views with 150 degrees on the horizontal axis and 50 mm (1.97 in.) on the vertical axis. The maximum and mean amplitude responses were measured in a region approximated by the box in each top view. The maximum responses at 77.4 and 79.4 full scale were within 0.23 dB of each other while the mean responses at 54.5 and 55.0 full scale differed by 0.079 dB. Typically calibration data that fall within ±2 dB of each other are acceptable so the equipment functionality was validated.

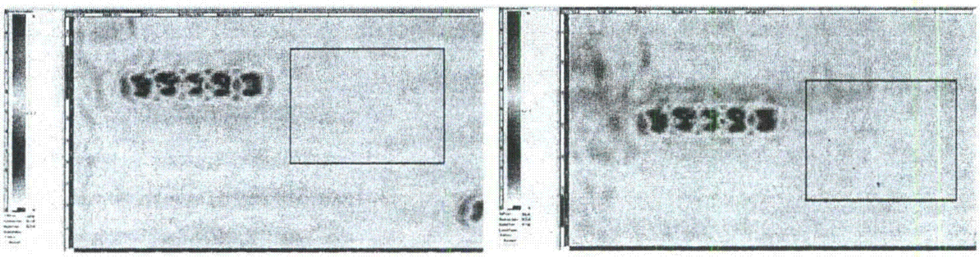

Figure 5.1 Calibration Data on the Blank Nozzle Piece Before (left) and After (right) Transport to RPL/33. The horizontal axis represents 150 degrees of circumference and the vertical axis represents 50 mm (1.97 in.) in the axial direction in each image.

Comment [PGO22]: Don't need all the description and figure. Just can say that the scanner functionality was validated after moving.

After equipment verification, the scanner was placed on Nozzle 63 in the glove bag as depicted in Figure 5.2 and diagrammed in Figure 5.3. The wetted side of the nozzle assembly was facing down. A plug was inserted in the wetted side of the nozzle several months earlier. At that time the nozzle was removed from storage and the length of nozzle extending above the reactor pressure vessel (RPV) head material (dry side) was shortened to give easier access to the interference fit region and for easier maneuvering of the nozzle/head assembly. Water was added several days prior to mounting the scanner on the nozzle. With the scanner in place, the glove bag was examined for any leakage points in the bag walls and glove ports. No leaks were found and the glove bag was sealed. Any materials entering the glove bag from this point forward were passed through an access port in the bag wall.

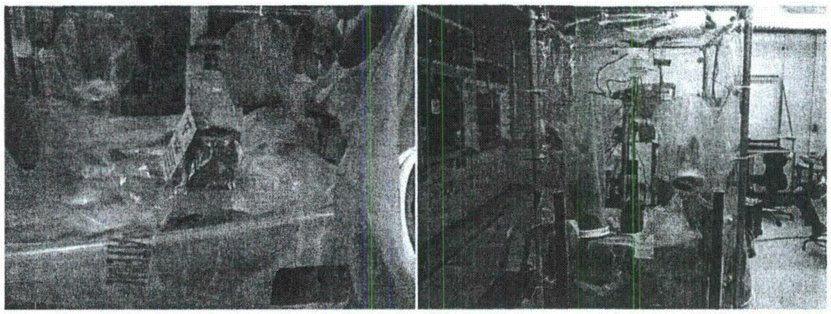

Figure 5.2 Dry Side of Nozzle 63 Prior to Scanner Mounting (left); Scanner Mounted on the Nozzle in the Glove Bag (right)

Comment [PGO23]: Same as Figure 3.9

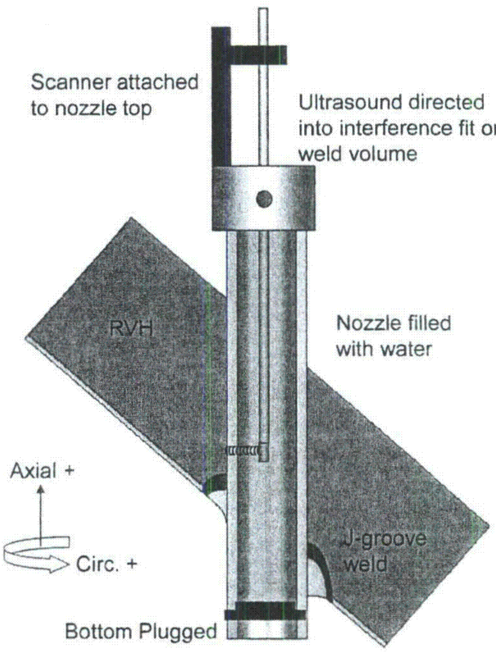

Figure 5.3 Schematic of Nozzle Assembly and Ultrasonic Evaluation of the Interference Fit

Comment [PGO24]: You have already used this image (Fig. 3.8). Do not repeat it. Reference previous figure if necessary.

5.2 Data Acquisition

Comment [PGO25]: This section does not need to include an extended discussion of the "bad" data. It is sufficient to say very briefly in text that first scan showed probe to be dirty so it was cleaned, second scan had problem with bubbles so they were brushed out. Then just present the good data.

Before the start of a scan, the probe was manually lowered to the bottom of the interference fit region and the data were collected while indexing the probe upwards. Two data channels were recorded during acquisition—one with a focus at the front surface (1 mm or 0.04 in.) and the other focused at the interference fit interface (15 mm or 0.59 in.). The front surface reflection represented the interface between the water inside the tube and the Alloy 600 tube inner diameter (ID), and provided an indication of the surface condition of the tube. This data would reveal bubbles, pitting, and other surface anomalies, if present. The second data channel recorded the reflection from the interface between outer diameter (OD) of the Alloy 600 tube and the carbon steel RPV head material, and represented the interference fit region. The first coarse scan data showed the need to laterally adjust the scanner to more accurately center the phased-array probe in the nozzle. Results from data acquired towards the top of the tube before and after centering the scanner are displayed in Figure 5.4. The horizontal axes in each image represent a circumferential distance from −90 to +90 degrees. The vertical axes represent approximately 20 mm (0.79 in.) of travel in depth or distance from the probe. Before centering the scanner, the front surface signal travel or difference from high to low point was measured at 10 mm (0.39 in.) on the left image. After centering, the signal travel was only 1 mm (0.04 in.) with the data displayed on the right of Figure 5.4. In addition to showing centeredness of the probe, the coarse scans also verified that the areas of interest were captured in the data file.

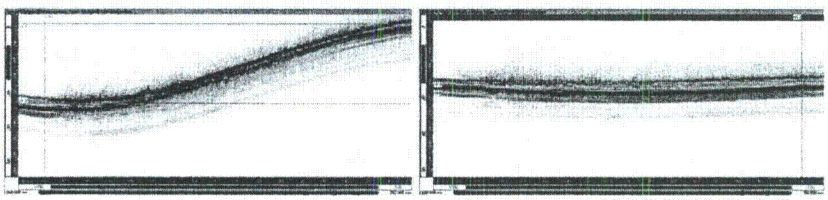

Figure 5.4 Alloy 600 Tube ID Response Before (left) and After (right) Centering the Scanner on the Nozzle. The horizontal axis represents approximately 180 degree and the vertical axis 20 mm (0.79 in.).

Comment [PGO26]: You don't need this figure. Just say that the probe was centered.

Once the areas of interest were bounded, the scanner step sizes were reduced for more detailed imaging. A resolution of 0.5 degree in the circumferential (scan) direction and 0.5 mm (0.02 in.) in the axial (index) direction were selected. The ZETEC UltraVision software limits the data files to 1 gigabyte in size. Working within this constraint, data in a file were collected over a range of approximately 180 degrees circumferentially and 380 mm (14.96 in.) axially. A previous examination of Nozzle 63 by industry indicated a leakage path at the low point or downhill side of the nozzle, which is the 180-degree location on the coordinate system established for this investigation. Therefore, data were acquired over an approximate −90 to +90 degree region and a 90 to 270 degree region to capture the possible leakage path in the center of an image. The actual circumferential scan regions were slightly larger than 180 degrees to provide some overlap in the data.

The first data covering the 90 to 270 degree area are shown in Figure 5.5. The front surface echo is displayed on the top and the interference fit echo on the bottom. These C-scan top view images show approximately 180 degrees across the horizontal axis and 360 mm (14.17 in.) on the vertical axis. The color bar on the left shows low-amplitude signals in blue/white, which represent good transmission or poor reflectance. High-amplitude signals in orange/red conversely represent poor transmission and good reflectance. The weld region is shown in the white-to-light-blue color at the bottom of the interference fit image. The interference fit or shrink-fit zone is located between the counter bore regions as was shown in Figure 1.1. The data above the interference fit (dry-side annulus region) represent a tube-to-air interface and should provide a strong and uniform reflection. Such a strong reflection was only evident in the orange-colored regions in the right side of the images. The tube OD-to-air interface is a good reflector, so a uniform orange color would be expected across the top of the image. Therefore, the lack of uniformity across the upper portion of the image (tube OD) was unexpected. The lack of uniformity across the entire front surface echo (upper image in the figure) was also unexpected.

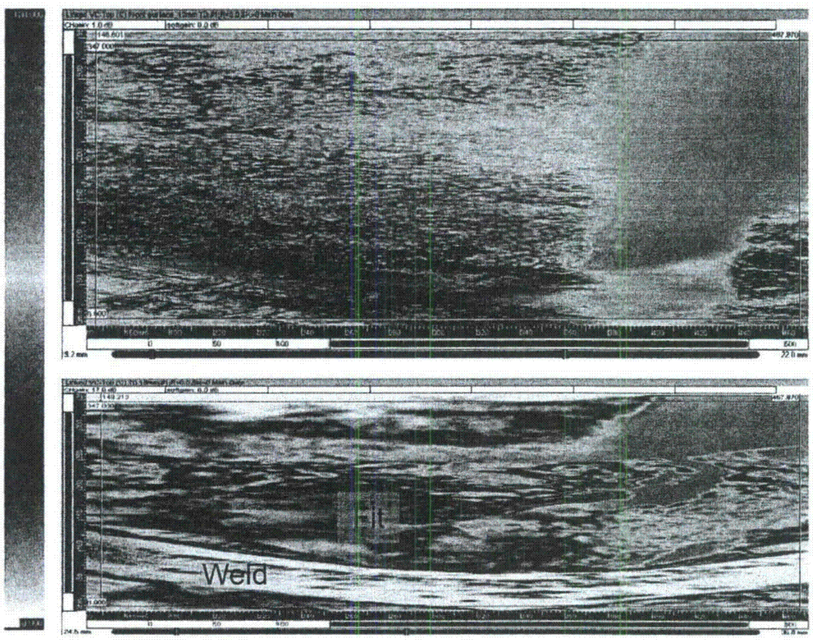

Figure 5.5 **First PA Ultrasonic Data from Nozzle 63. The front surface or nozzle ID echo is on the top and the interference fit echo on the bottom. The horizontal axis represents the 86 to 274 degree area and the vertical axis represents 360 mm (14.17 in.). The color scale is represented on the far left.**

Comment [PGO27]: Remove figure

After the first scanning attempt, the probe was lifted above the water line and found to be dirty. The probe face was carefully wiped with a dry cloth. It was also suspected that bubbles on the ID tube surface could be partly responsible for the degraded image. Since the presence of bubbles in the tube could not easily be visually confirmed, a metal rod was swiped around the ID surface in an attempt to dislodge and remove any bubbles. Thereafter, the next set of data, given in Figure 5.6, were acquired and showed an improvement in the uniformity of the OD tube echo above the interference fit, as seen in the lower image. A possible leakage path was also detected starting at the weld near the 180 degree or low position and extending upwards and to the right. Bubbles on the ID tube surface were still suspected in the front surface data shown in the top image. These were confirmed in data acquired from the front surface echo over a small region. The data are displayed in Figure 5.7 with multiple bubbles noted and the lack of uniformity in amplitude response still evident.

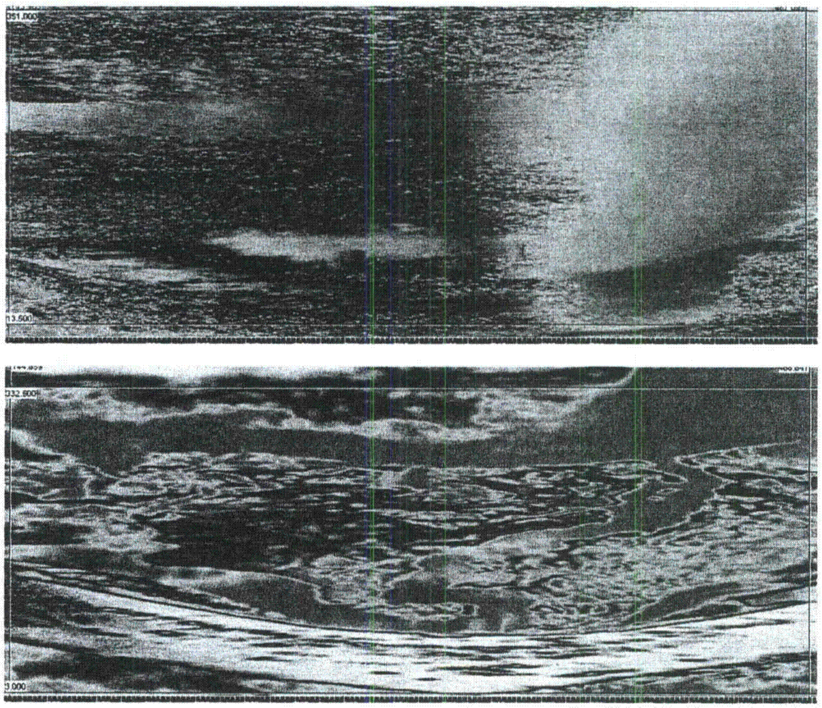

Figure 5.6 **PA Ultrasonic Data from Nozzle 63 Acquired After Cleaning the Probe Face. The front surface or nozzle ID echo is on the top and the interference fit echo on the bottom. The horizontal axis represents the 86 to 274 degree area and the vertical axis represents 360 mm (14.17 in.).**

Comment [PGO28]: Remove figure.

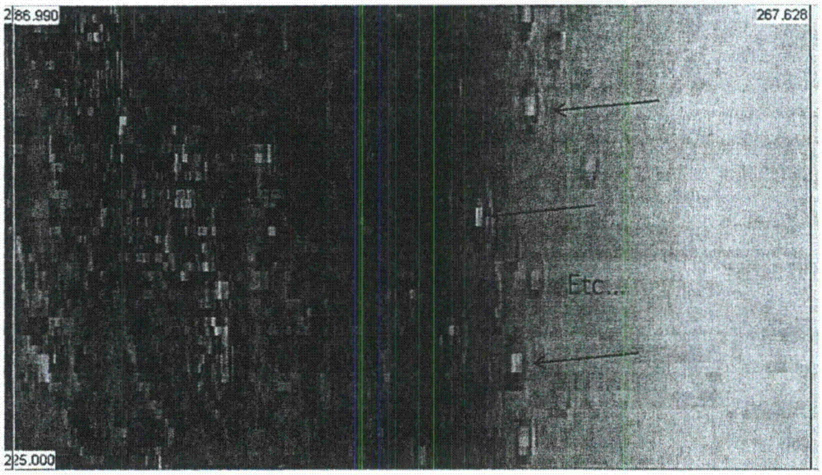

Figure 5.7 Bubbles are Detected on the ID of the Nozzle, some of which are Indicated by Arrows. The vertical axis represents 25 mm (0.98 in.) and the horizontal axis represents 190 degrees.

Comment [PGO29]: Remove figure.

After this second scan attempt, it was decided to brush the tube ID surface to remove bubbles but to do it carefully to minimize or avoid introducing new bubbles. The top photo in Figure 5.8 shows the brush being inserted past the probe and into the nozzle. The bottom photo is another view of the manual brushing process. The data acquired after brushing are shown in Figure 5.9 with the front surface echo on top and the interference fit data on the bottom. Several days later the tube ID was brushed again and data acquired to show repeatability of the data and to attempt to remove any remaining bubbles. These results are depicted in Figure 5.10. As expected, the interference fit image (bottom image) showed nearly uniform amplitude response from the tube OD above the interference fit (orange region at top of image). More bubbles were removed during the second brushing as evidenced by the smoother front surface image on the top in Figure 5.10 as compared to Figure 5.9.

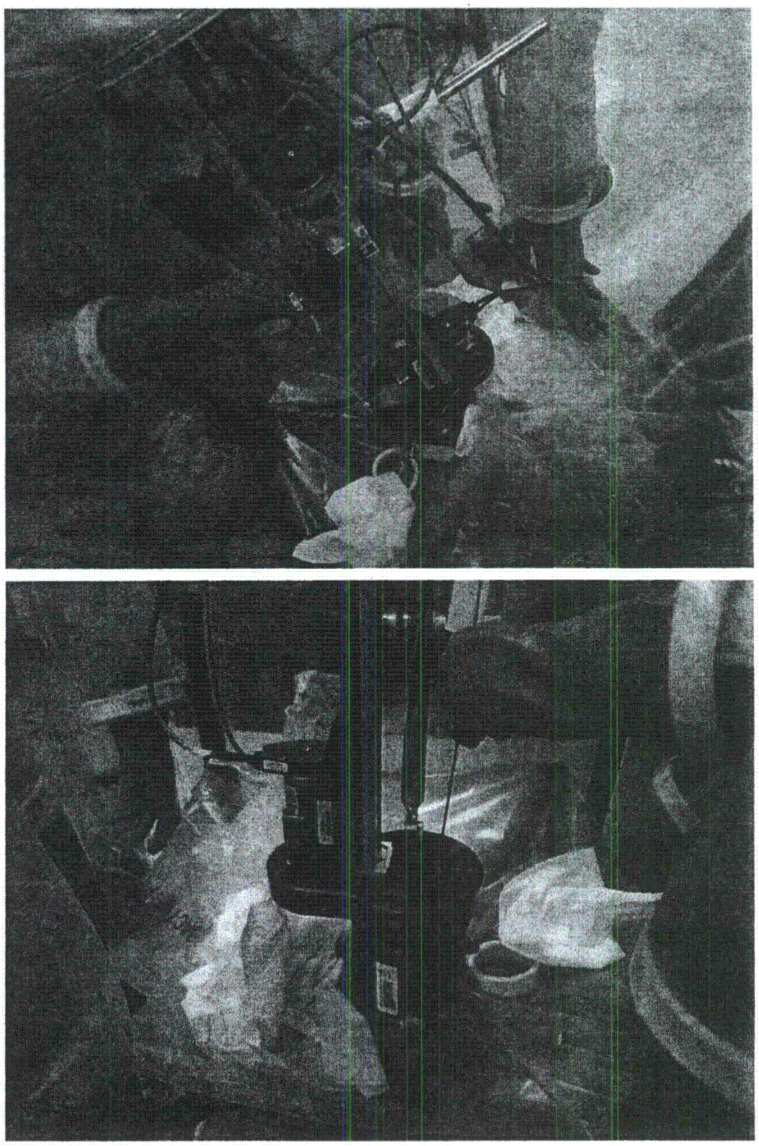

Figure 5.8 Brush Used to Remove Surface Bubbles (top); Brushing in Progress (bottom)

Comment [PGO30]: Remove figure.

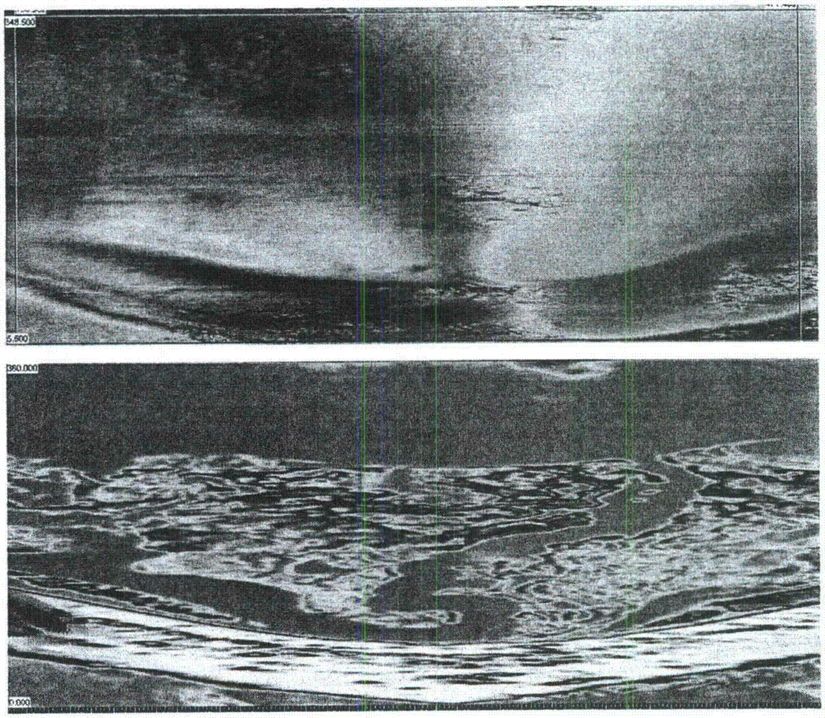

Figure 5.9 PA Ultrasonic Data from Nozzle 63 Acquired After First Brushing of the Nozzle ID. The front surface or nozzle ID echo is on the top and the interference fit echo on the bottom. The horizontal axis represents the 86 to 274 degree area and the vertical axis represents 360 mm (14.17 in.).

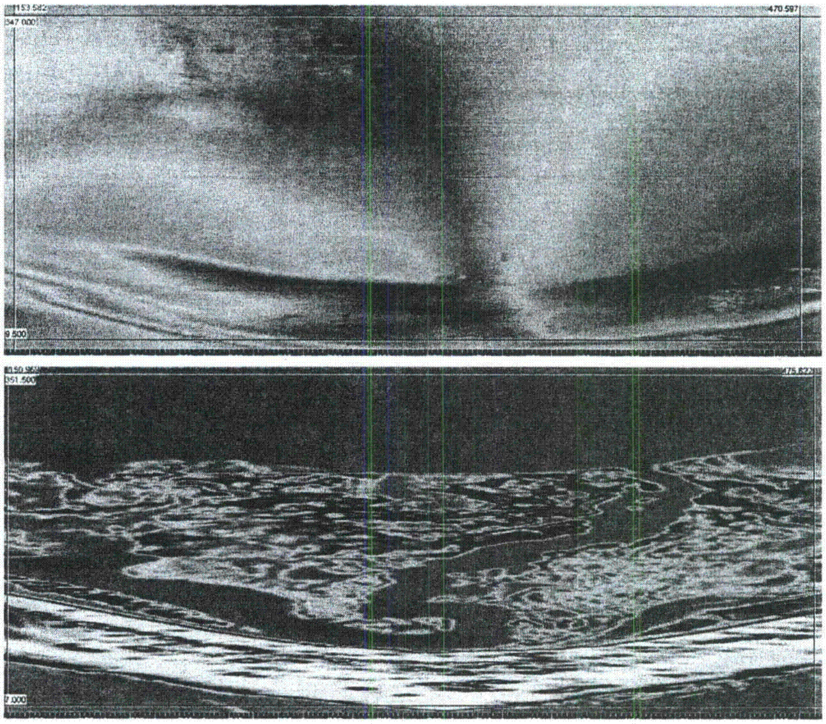

Figure 5.10 **PA Ultrasonic Data from Nozzle 63 Acquired After Second Brushing of the Nozzle ID. The front surface or nozzle ID echo is on the top and the interference fit echo on the bottom. The horizontal axis represents the 86 to 274 degree area and the vertical axis represents 360 mm (14.17 in.).**

Comment [PGO31]: Remove figure.

Data acquired after the first brushing from the two scans were pieced together to form the composite image of the interference fit region in Figure 5.11. This image displays a full 360-degree representation of the weld and interference fit region with −90 degrees at the left and 270 degrees at the right. The suspected leakage path at the low point, near 180 degrees, is marked with arrows. Also observed from the weld region response are suspected inclusions or fabrication flaws. Several of these indications are circled in red in the figure.

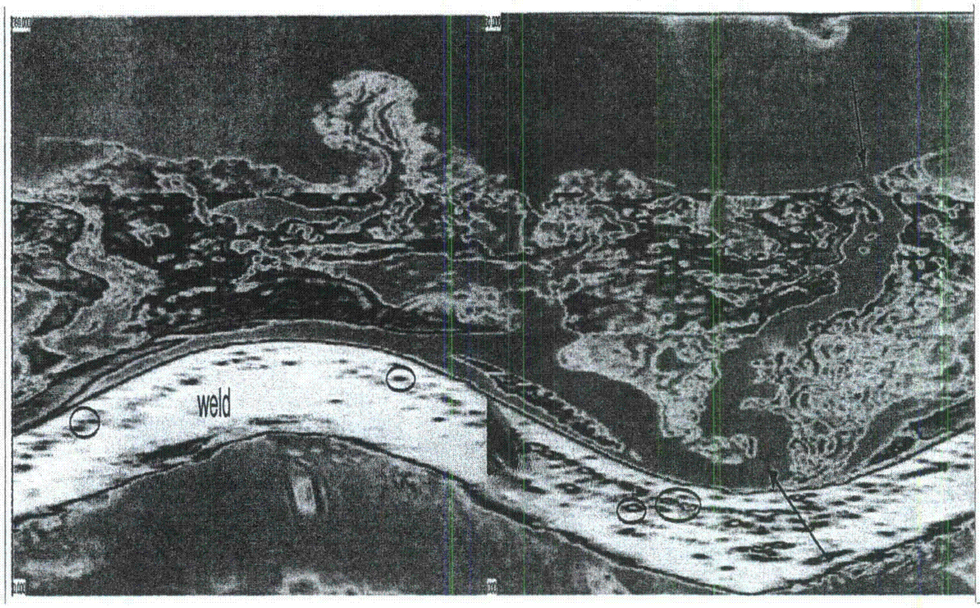

Comment [PGO32]: This is the important figure. Everything in the chapter up to this can be described by a few paragraphs of text at most.

Figure 5.11 **PA Ultrasonic Data from the Interference Fit in Nozzle 63 Acquired After the First Brushing of the Nozzle ID. The horizontal axis represents the full 360-degree area and the vertical axis represents 360 mm (14.17 in.).**

Comment [PGO33]: Say that the arrows indicate the main leakage path. Don't circle the indications. Leave those for the section on the weld analysis. Maybe identify -90 on left and 270 on right for reference.

5.3 Amplitude Analysis

An analysis based on amplitude responses was conducted on the data images. The first such analysis was conducted on the 90 to 270 degree data acquired after the first brushing. The image was segregated into regions as depicted in Figure 5.12. The peak and mean amplitude responses were measured in each boxed region. Regions 1 through 6 are suspected leakage path zones. Regions 7 through 10 represent the interference fit and lower counter bore areas. Regions 11 through 15 represent the tube above the interference fit, and regions 16 through 18 represent the interference fit with suspected boric acid present. The same procedure was used on the −90 to +90 degree data with the boxed regions shown in Figure 5.13. Finally, the mean amplitudes within each boxed region were plotted against the box numbers with results in Figure 5.14. The suspected leakage path and tube responses all were in the range of 60 percent of full screen height and greater. At the other extreme, the regions with suspected boric acid deposits had mean amplitudes 25 percent and below. Finally, the interference fit/counter bore region mean amplitudes were in the 41 to 58 percent range. A proposed segregation of the regions is denoted by the yellow, green, and blue colored zones in the plot. The data suggest that 30 percent mean amplitude or less indicates the presence of boric acid in the interference fit while greater than 60 percent represents an air gap and possible leakage path if connected all the way through (top to bottom) the interference fit. Note that the same analysis

Comment [PGO34]: Make clear that the justification for suggesting that Region 1-6 is leakage path, Region 7-10 is interference fit, etc. is from the mockup results. Say that these suggestions need to be confirmed by destructive analyses.

was performed on the data acquired after the second brushing, to remove bubbles, and produced similar results. In a direct comparison of data values, the difference was 2 percent or less in mean response, indicating the data are similar in response amplitudes from the segregated zones.

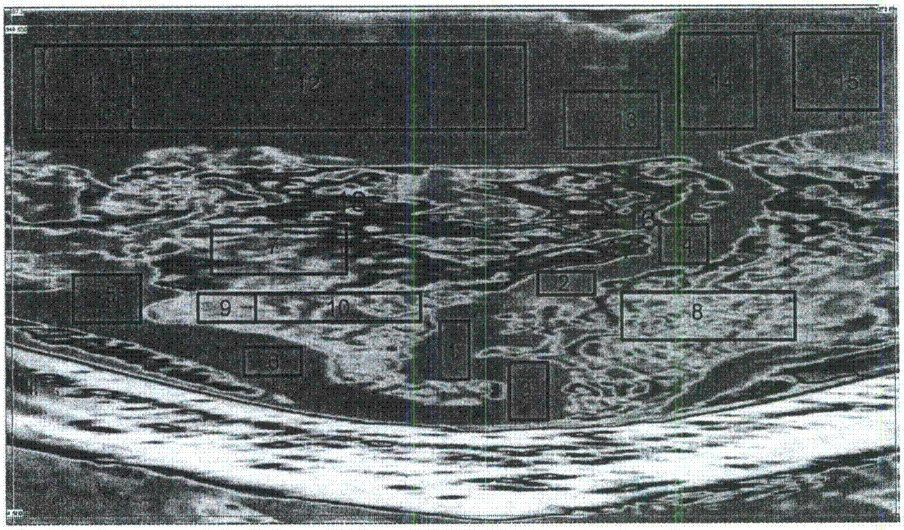

Figure 5.12 Interference Fit Data Image After First Brushing. The horizontal axis represents approximately 90 to 270 degrees. The vertical axis represents 360 mm (14.17 in.).

Comment [PGO35]: Say that the boxes correspond to regions for the amplitude analysis.

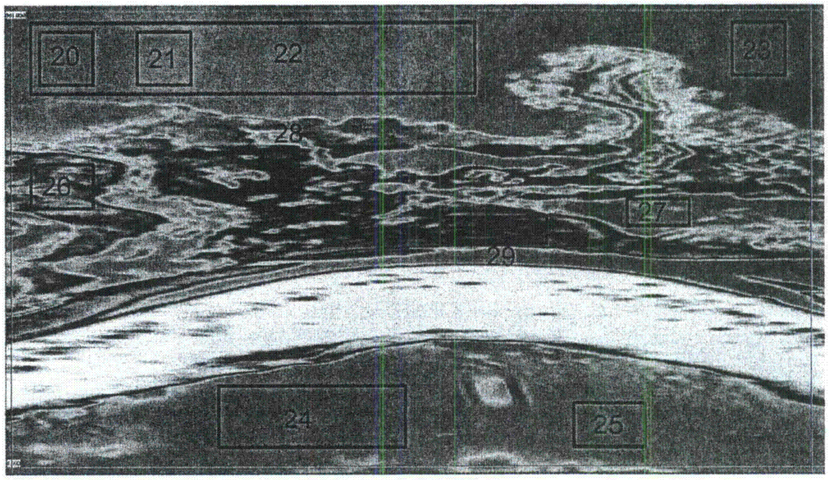

Figure 5.13 Interference Fit Data Image After First Brushing. The horizontal axis represents approximately −90 to +90 degrees. The vertical axis represents 360 mm (14.17 in.).

Comment [PGO36]: See comment above.

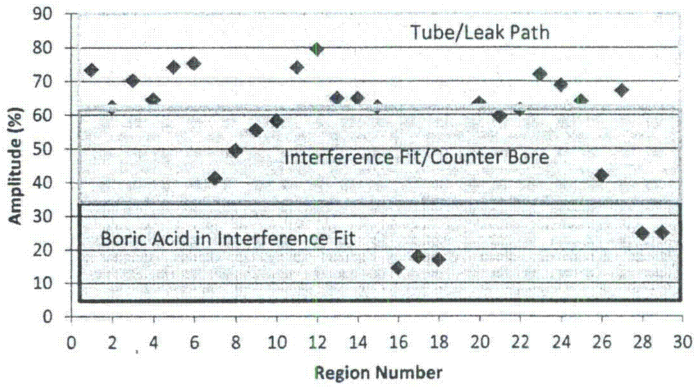

Figure 5.14 Mean Amplitude Response from the Regions Indicated in Figures 5.12 and 5.13

Comment [PGO37]: This plot needs to be changed to better display the data. At a glance it looks like a random scatter of points because the region number has no correspondence to the amplitude. For example, it might display better if Regions 1-5 were selected as low amplitude locations,, Regions 6-12 were selected as intermediate amplitude, etc.

In summary, the mean amplitude responses from the different regions in the data image were measured. Based on this analysis, the regions are separable and compare favorably to the responses measured previously on the calibration mockup specimen. A comparison of the responses is presented in Table 5.1. Note that the Nozzle 63 data were acquired with 1 dB more gain (13 dB as opposed to 12 dB) than the calibration mockup data and this difference was accounted for in the analysis.

Table 5.1 Mean Amplitude Responses (%)

Region	Calibration Mockup	Nozzle 63
Tube/Leak Path	60–75	60–79
Interference Fit/Counter Bore	40–55	41–58
Interference Fit – with Boric Acid	24–30	14–25

In a color-coded qualitative sense, the C-scan image analysis is also divided into three categories. The orange color implies that an air gap exists in the interference fit or counter bore response and presents a large reflected signal. Orange also represents the tube response outside of the interference fit region. The interference fit and counter bore regions with some contact between the tube OD and the low alloy steel are represented by the green-to-yellow colors and the interference fit region with greater contact is represented by the blue-to-white colors. This greater contact is assumed to be due to the presence of boric acid. Destructive analyses are needed to confirm these results.

A composite view of the data acquired after the second brushing is presented in Figure 5.15. This is the best representation of the interference fit region and from this data a cut was selected for destructive evaluation.

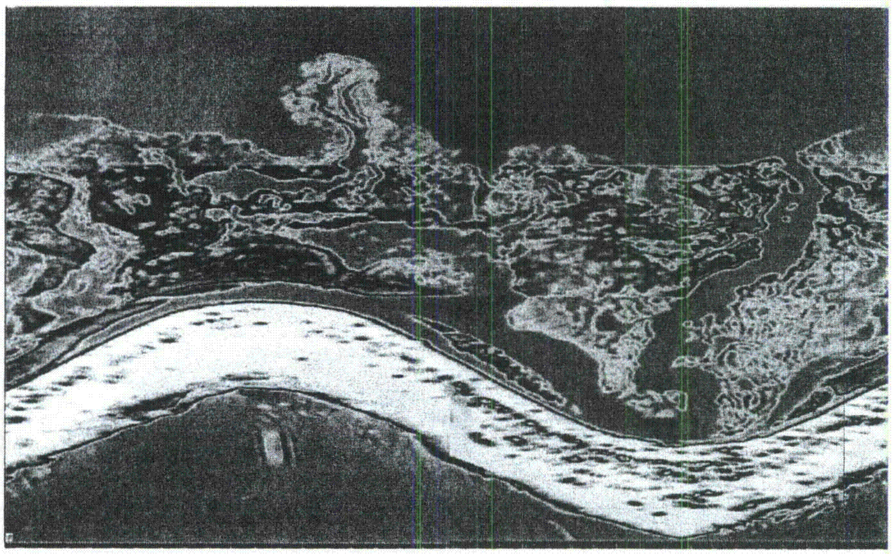

Figure 5.15 Nozzle 63 Interference Fit Data After Second Brushing. The horizontal axis represents −95 to 275 degrees. The vertical axis represents 360 mm (14.27 in.).

Based on the amplitude analyses conducted, the data were also plotted with a tri-level color bar to represent the three categories previously discussed. The tri-level color bar implementation is shown in Figure 5.16. White represents the less than 30% amplitude range and indicates good transmission such as in the weld or possible boric acid in the interference fit region. Light blue represents the 30 to 60% amplitude range and indicates the interference fit and counter bore regions. Dark blue represents the above 60% amplitude range and indicates poor transmission such as in the tube above the interference fit or an air gap in the interference fit and counter bore regions. A leakage path exists if a gap in the interference fit region extends fully through the interference fit connecting the weld and annulus region immediately above the weld to the dry side of the tube. From this image as well as the rainbow color-coded images, one clear leakage path is visible. The leakage path starts in the vicinity of 180 degrees circumferentially, or the low point of the nozzle, and meanders upwards and toward the right in the image. Other leakage paths are also evident but may not connect all the way through to the dry side of the assembly. Destructive analyses are needed to confirm the cause of these regions of differing reflectivity.

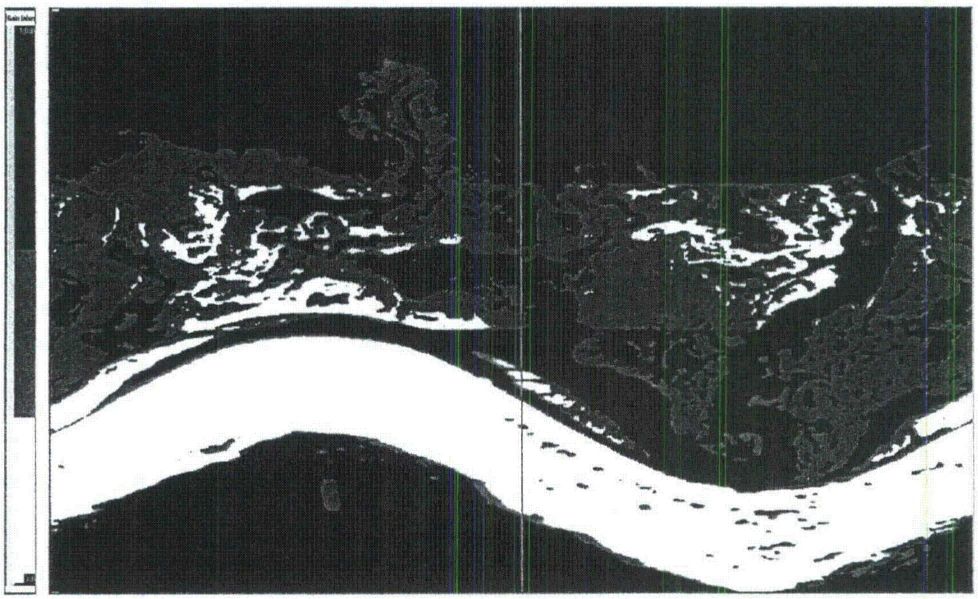

Figure 5.16 A Tri-Color Representation of the Interference Fit Data

Comment [PGO38]: You may state what the 3 colors represent.